Numerical Simulations of Type Ia Supernovae

Andy Nonaka
Lawrence Berkeley National Laboratory
January 19, 2011

Outline

- Motivation: Type Ia Supernovae (SNe Ia)
- MAESTRO: Low Mach Number Astrophysics
  - Algorithmic Details
  - Scientific Results
  - Transition to Compressible Framework
- Primary Collaborators
  - Ann Almgren, John Bell, Mike Lijewski, Candace Gilet: LBNL
  - Mike Zingale, Chris Malone: Stony Brook University

Motivation: Type Ia Supernovae

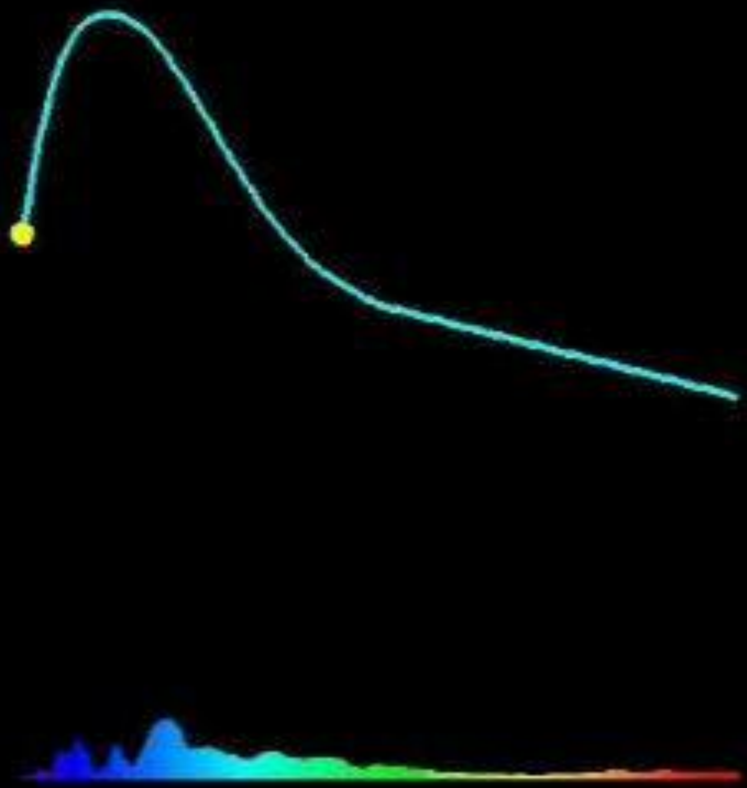

- Using modern telescopes, Type Ia supernova light curves can now be observed several hundred times per year:
  - Spectra contains silicon, lacks hydrogen
  - Peak powered by radioactive decay of nickel

Type Ia Supernovae are Distance Indicators

- Observation: SNe Ia light curves have the same shape, differing only by the decay rate of the light cure.
- Fact: The relative brightness and the decay rate of the light curves are related in a calculable manner: wider = brighter.
- Conclusion: By observing the peak luminosity and decay rate, we can determine the distance to the host galaxy.

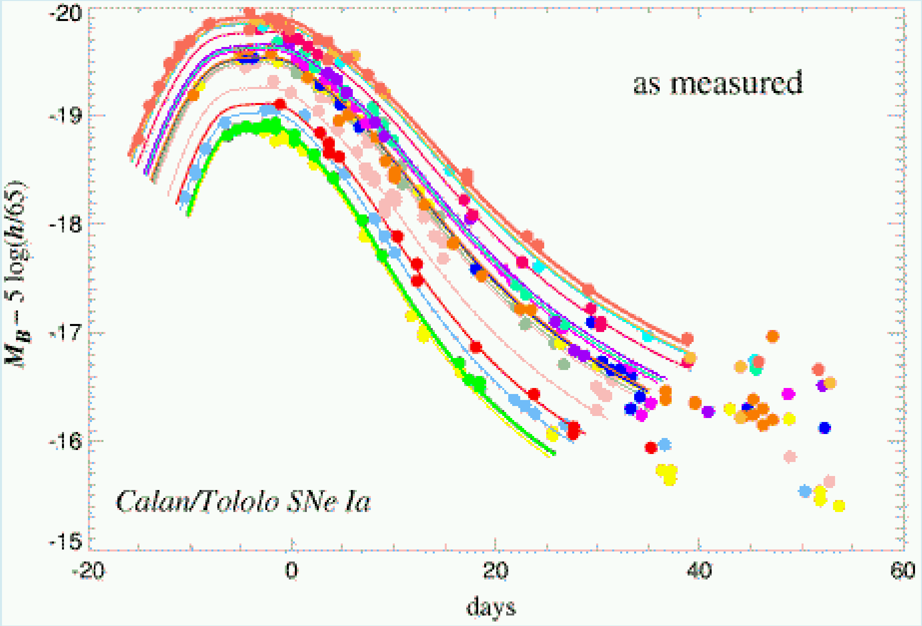

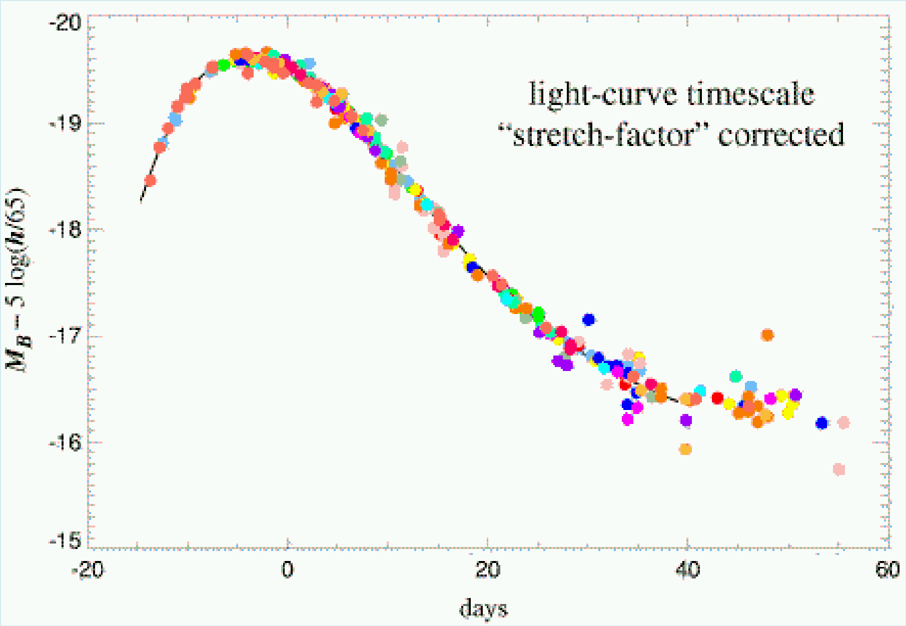

Type Ia Supernovae are Speed Indicators

- Due to the observed redshift, we know the speed at which the host galaxy is moving away from us.
  - Led to discovery of the acceleration of the expansion of the universe (1998)
- We require a better theoretical understanding of SNe Ia!!!
  - Use computation to validate theory

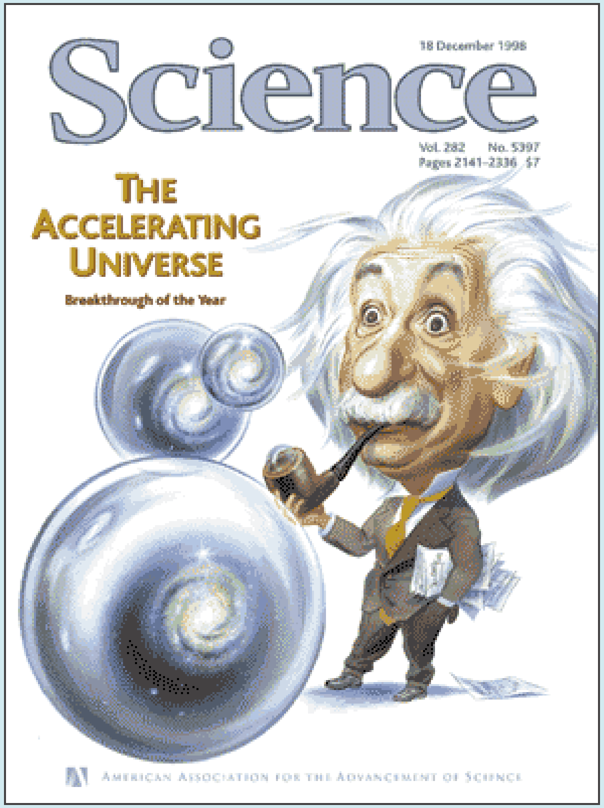

The Phases of Type Ia Supernovae

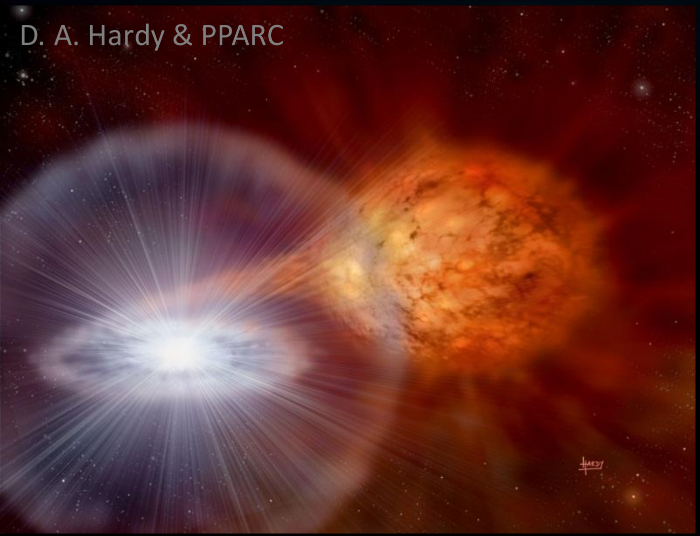

A white dwarf accretes matter from a binary companion over millions of years.

Smoldering phase characterized by subsonic convection and gradual temperature rise lasts hundreds of years.

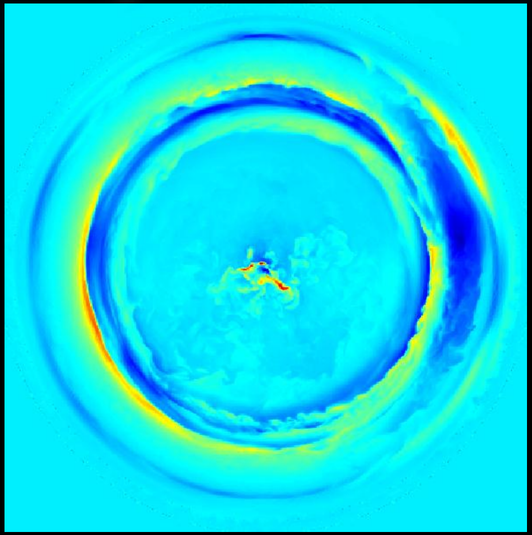

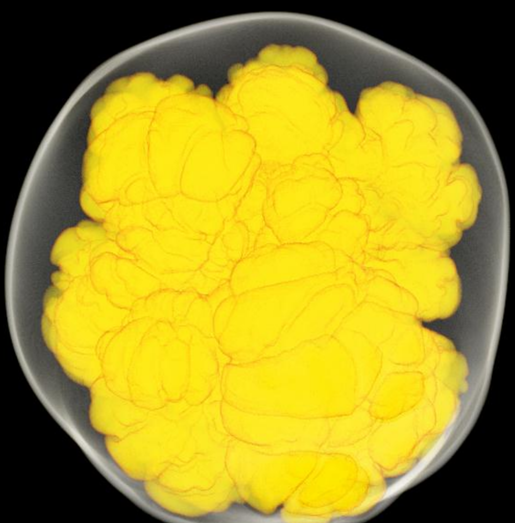

Haitao Ma, UCSC

Flame (possibly) transitions to a detonation, causing the star to explode within two seconds.

The resulting event is visible from Earth for weeks to months.

SN 1994D (High-Z SN Search team)

Each Phase has Different Computational Requirements

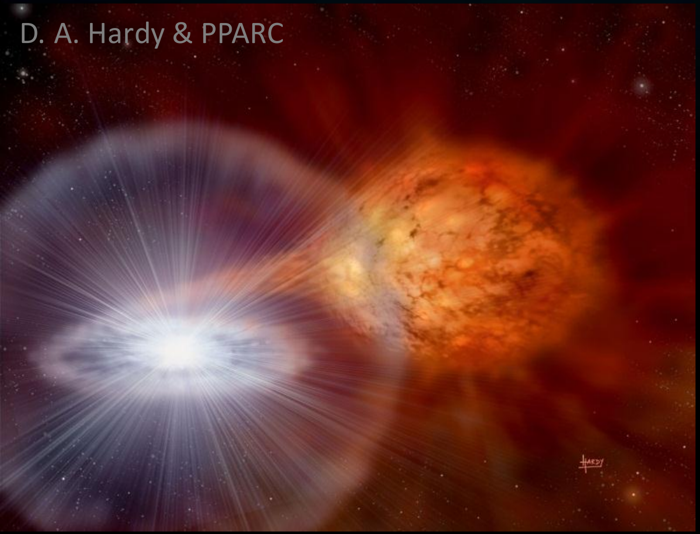

KEPLER
(Woosley, UCSC)

MAESTRO
(CCSE)

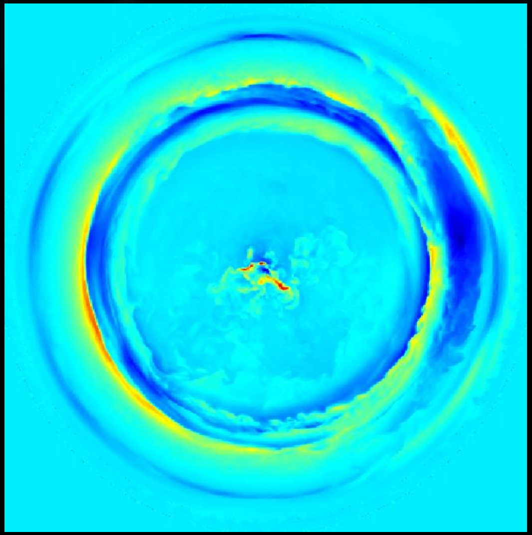

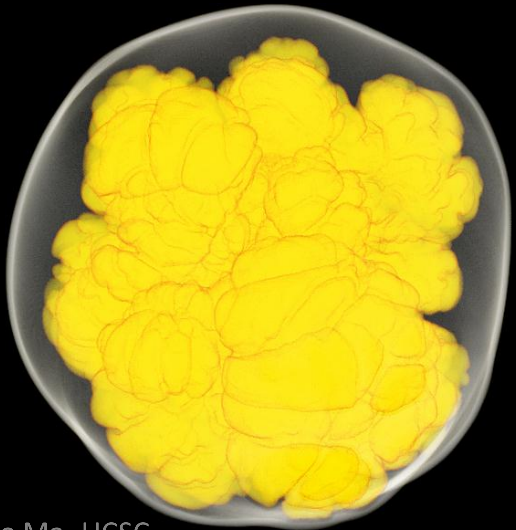

Haitao Ma, UCSC

CASTRO
(CCSE)

SEDONA
(Kasen, Nugent, Thomas, LBNL)

SN 1994D (High-Z SN Search team)

Computing the Convective Phase

MAESTRO
(CCSE)

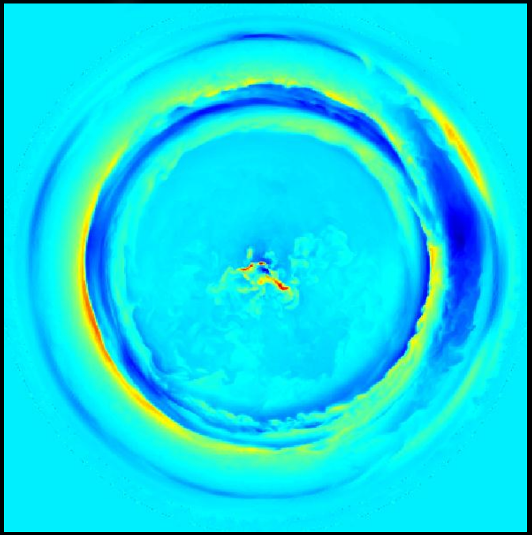

- We are particularly interested in the last few hours of convection preceding ignition.
  - Low Mach number regime; $M = U/c$ is $O(10^{-2})$
  - Long-time integration infeasible using fully compressible approach
  - We wish to use MAESTRO to determine the initial conditions for the detonation / explosion phase for CASTRO
    - Previous studies have artificially seeded hot ignition points into their initial conditions

MAESTRO: Low Mach Number Astrophysics

- Algorithmic Details

What is MAESTRO?

- MAESTRO is a massively parallel, finite volume, adaptive mesh refinement (AMR) code for low Mach number astrophysical flows (Fortran90 BoxLib).
- Equation set derived using low Mach number asymptotics
  - Looks similar to the standard equations of compressible flow, but sound waves have been analytically removed
    - Enables time steps constrained by the fluid velocity CFL, not the sound speed CFL:

$$\Delta t_{\mathrm{compressible}} < \frac{\Delta x}{|u| + c} \qquad \Delta t_{\mathrm{lowMach}} < \frac{\Delta x}{|u|}$$

    - Low Mach time step is a factor of 1/M larger, enabling long-time integration

MAESTRO Features

- No acoustic waves
  - Allows for large time steps
- Retain local compressibility effects
  - Reactions, thermal diffusion, and external heating
- Highly stratified atmospheres
  - Density and pressure span many orders of magnitude
  - Time dependent: captures expansion
- General equation of state
- Model full spherical stars
- AMR
- Scales scientific production jobs to 100K cores

MAESTRO Equation Set

- Using low Mach number asymptotics, the pressure can be decomposed into a base state and perturbational component:

$$p(\mathbf{x},t) = p_0(r,t) + \pi(\mathbf{x},t); \qquad \frac{\pi}{p_0} = \mathcal{O}(M^2)$$

- We define a base state density, ρ_0, that represents the average density as a function of radius and time.
  - Base state pressure is determined by hydrostatic equilibrium:

$$\nabla p_0(r,t) = -\rho_0(r,t)|\mathbf{g}|$$

gravity

- Key point: by replacing p with p_0 everywhere except the momentum equation, we analytically remove acoustic waves from our system.

MAESTRO Equation Set

- Conservation of mass, momentum, and energy:

$$\begin{aligned}\frac{\partial(\rho X_k)}{\partial t} &= -\nabla\cdot(\rho X_k \mathbf{u}) + \rho\dot{\omega}_k \\ \frac{\partial(\rho \mathbf{u})}{\partial t} &= -\nabla\cdot(\rho \mathbf{u}\mathbf{u}) - \nabla\pi - (\rho-\rho_0)\mathbf{g} \\ \frac{\partial(\rho h)}{\partial t} &= -\nabla\cdot(\rho h \mathbf{u}) + \frac{Dp_0}{Dt} + \nabla\cdot k_{\mathrm{th}}\nabla T + \rho H\end{aligned}$$

ρ	density	h	specific enthalpy
$\mathbf{u}$	velocity	k_{th}	thermal diffusion coefficient
X_k	mass fraction of species “k”	H	Heating due to reactions and external sources
$\dot{\omega}_k$	reaction rate of species “k”		

- System is closed with an equation of state linking ρ, X_k, h, and p_0, which are to remain in thermodynamic equilibrium.

MAESTRO Equation Set

- Conservation of mass, momentum, and energy:

$$\frac{\partial(\rho X_k)}{\partial t} = -\nabla\cdot(\rho X_k \mathbf{u}) + \rho\dot{\omega}_k$$

$$\frac{\partial(\rho\mathbf{u})}{\partial t} = -\nabla\cdot(\rho\mathbf{u}\mathbf{u}) - \nabla\pi - (\rho-\rho_0)\mathbf{g}$$

$$\frac{\partial(\rho h)}{\partial t} = -\nabla\cdot(\rho h\mathbf{u}) + \frac{Dp_0}{Dt} + \nabla\cdot k_{\mathrm{th}}\nabla T + \rho H$$

- Equation of state is expressed as a divergence constraint, derived by integrating the equation of state along particle paths:

$$\nabla\cdot(\beta_0\mathbf{u}) = \beta_0 S$$

$$S = \frac{\sigma}{\rho}\nabla\cdot k_{\mathrm{th}}\nabla T - \sigma\sum_k \xi_k\dot{\omega}_k + \frac{1}{\rho p_\rho}\sum_k p_{X_k}\dot{\omega}_k + \sigma H + \frac{1}{\overline{\Gamma}_1 p_0}\frac{\partial p_0}{\partial t}$$

  - "S" captures local compressibility effects due to thermal diffusion, compositional changes, reaction and external heating.
  - $\beta_0(r,t)$ is a density-like variable that captures expansion due to stratification

MAESTRO Equation Set

- Conservation of mass, momentum, and energy:

$$\frac{\partial(\rho X_k)}{\partial t} = -\nabla \cdot (\rho X_k \mathbf{u}) + \rho\dot{\omega}_k$$

$$\frac{\partial(\rho \mathbf{u})}{\partial t} = -\nabla \cdot (\rho \mathbf{u}\mathbf{u}) - \nabla\pi - (\rho - \rho_0)\mathbf{g}$$

$$\frac{\partial(\rho h)}{\partial t} = -\nabla \cdot (\rho h \mathbf{u}) + \frac{Dp_0}{Dt} + \nabla \cdot k_{\mathrm{th}}\nabla T + \rho H$$

- Base state density evolves subject to its own evolution equation
  - $w_0(r,t)$ is the average outward velocity at a given radius

$$\frac{\partial \rho_0}{\partial t} = -\nabla \cdot (\rho_0 w_0 \mathbf{e_r}) - \nabla \cdot (\eta \mathbf{e_r})$$

expansion of atmosphere due to large-scale heating

expansion of atmosphere due to large-scale convection

Summary of Algorithmic Approach

- MAESTRO is a "12-step program"
  - Predictor-corrector approach: advance solution using low order approximation for "S", then update "S" and re-advance solution
- Strang splitting to couple the advection, diffusion, and reactions in a second-order projection method framework

$$
\begin{aligned}
\frac{\partial(\rho X_k)}{\partial t} &= -\nabla \cdot (\rho X_k \mathbf{u}) + \rho \dot{\omega}_k \\
\frac{\partial(\rho \mathbf{u})}{\partial t} &= -\nabla \cdot (\rho \mathbf{u}\mathbf{u}) - \nabla \pi - (\rho - \rho_0)\mathbf{g} \\
\frac{\partial(\rho h)}{\partial t} &= -\nabla \cdot (\rho h \mathbf{u}) + \frac{D p_0}{D t} + \nabla \cdot k_{\mathrm{th}} \nabla T + \rho H
\end{aligned}
$$

$$\nabla \cdot (\beta_0 \mathbf{u}) = \beta_0 S$$

Summary of Algorithmic Approach

- Advection uses second-order Godunov integrator
- Reactions computed with VODE stiff ODE integrator
- Thermal diffusion treated semi-implicitly (multigrid)
- Divergence constraint and pressure update uses projection method, requiring a variable-coefficient elliptic solve (multigrid)

$$\frac{\partial(\rho X_k)}{\partial t} = -\underline{\nabla \cdot (\rho X_k \mathbf{u})} + \underline{\rho \dot{\omega}_k}$$

$$\frac{\partial(\rho \mathbf{u})}{\partial t} = -\underline{\nabla \cdot (\rho \mathbf{u}\mathbf{u})} - \underline{\nabla \pi} - \underline{(\rho - \rho_0)\mathbf{g}}$$

$$\frac{\partial(\rho h)}{\partial t} = -\underline{\nabla \cdot (\rho h \mathbf{u})} + \underline{\frac{D p_0}{D t}} + \underline{\nabla \cdot k_{\mathrm{th}} \nabla T} + \underline{\rho H}$$

$$\underline{\nabla \cdot (\beta_0 \mathbf{u}) = \beta_0 S}$$

Base State Mapping

- What makes MAESTRO unique is the incorporation of a time-dependent, one-dimensional base state.
  - Evolve base state using 1D Godunov integrator
  - Frequent mapping from 1D to 3D and vice versa

$$
\begin{aligned}
\frac{\partial(\rho X_k)}{\partial t} &= -\nabla \cdot (\rho X_k \mathbf{u}) + \rho \dot{\omega}_k \\
\frac{\partial(\rho \mathbf{u})}{\partial t} &= -\nabla \cdot (\rho \mathbf{u}\mathbf{u}) - \nabla \pi - (\rho - \rho_0)\mathbf{g} \\
\frac{\partial(\rho h)}{\partial t} &= -\nabla \cdot (\rho h \mathbf{u}) + \frac{D p_0}{D t} + \nabla \cdot k_{\mathrm{th}} \nabla T + \rho H
\end{aligned}
$$

$$
\nabla \cdot (\beta_0 \mathbf{u}) = \beta_0 S
$$

Base State Mapping

- Visually, here is how the base state is related to the full state

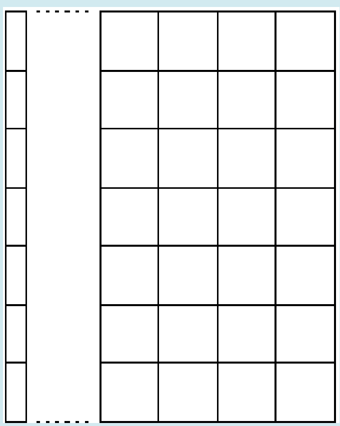

"planar" problems

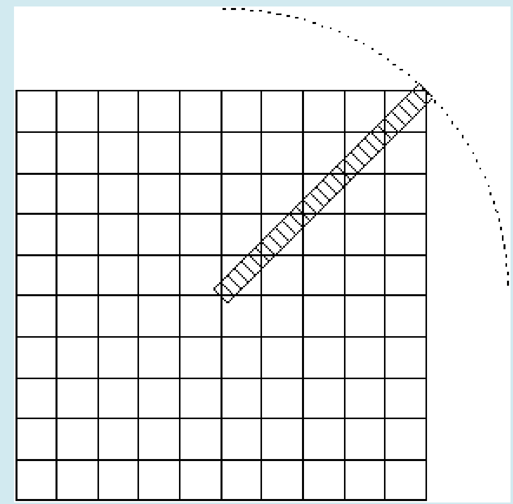

"spherical" problems

- Note that for spherical problems, there is no direct alignment between the 1D base state array and the full state.

Spherical "Fill" Operator

- For spherical problems, mapping from the base state to the full state can be done using quadratic interpolation.
  - We define a "fill" operator.

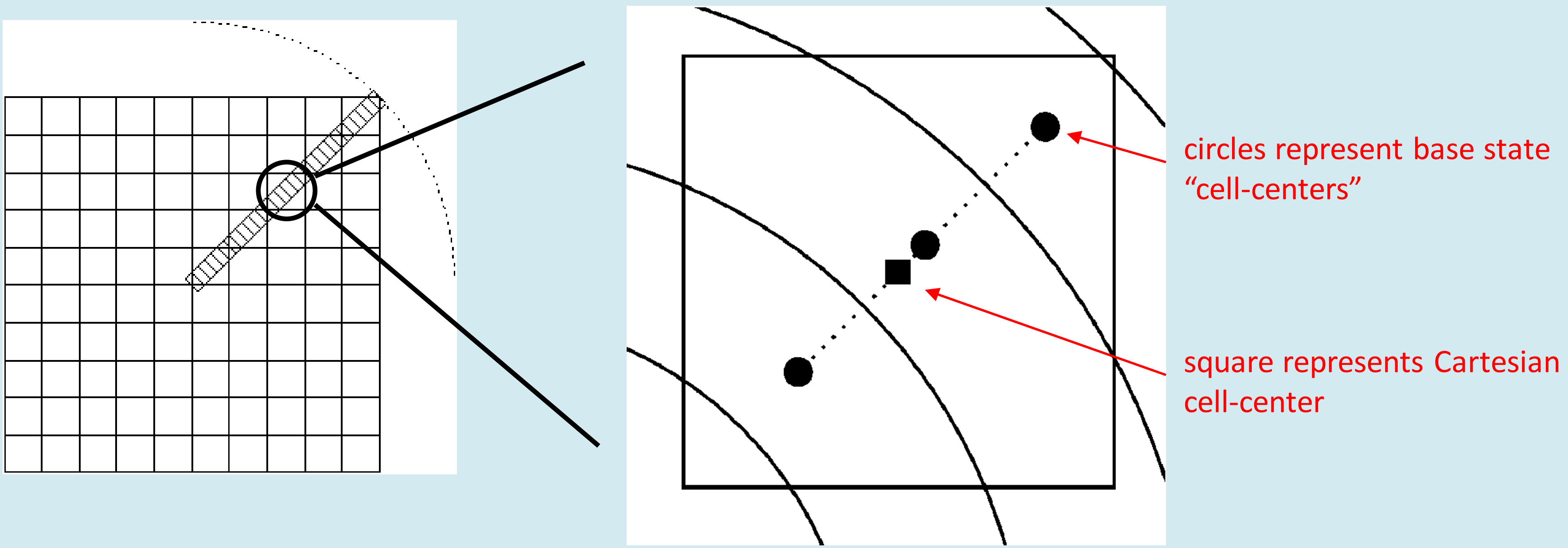

- The base state grid spacing must be chosen to be smaller than the full state grid spacing.
  - We have discovered that $\Delta r = (1/5)\,\Delta x$ gives sufficient accuracy in our mapping tests

"Average" Operator

- Mapping from the full state to the base state requires more care.
  - We define an "average" operator.

- Computing the average is straightforward for planar problems since there is direct alignment between the Cartesian grid and the base state.

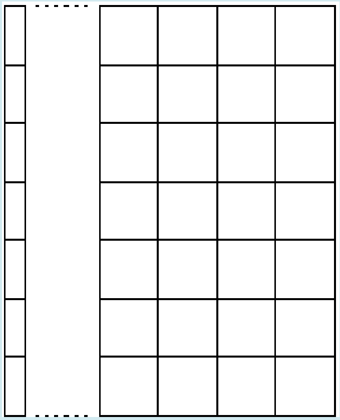

- Spherical problems are more complicated since there is no direct alignment.

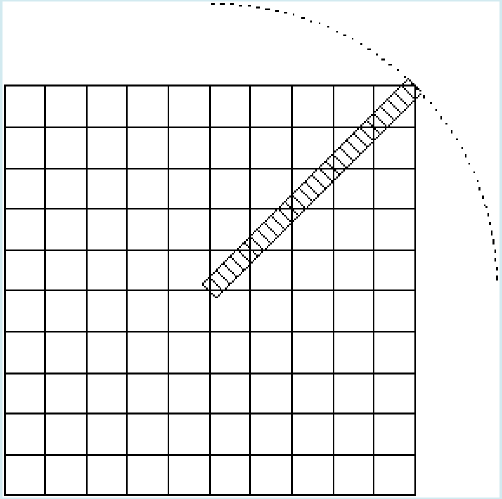

Spherical Average Operator

- Simply averaging the cell values that directly map to a particular radial bin is not accurate enough.
  - As a test, we map a 1D Gaussian profile onto a 384^3 domain, and then "average" the Cartesian grid state onto a 1D array.
  - Plot below shows the relative error is $O(10^{-4})$ – not accurate enough.

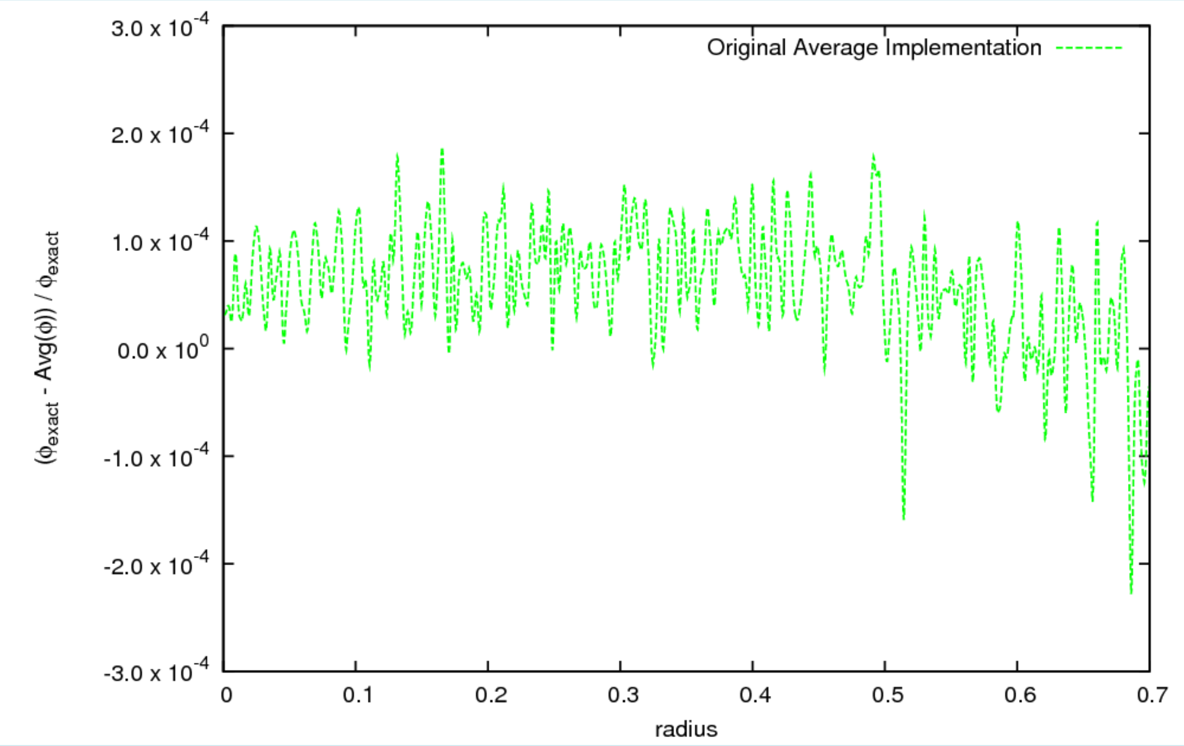

Spherical Average Operator

- We note that every Cartesian cell center must be at a radius r_m from the center of the star (m is an integer):

$$r_m = \Delta x \sqrt{0.75 + 2m}$$

Hit Count Chart for a 384^3 Domain

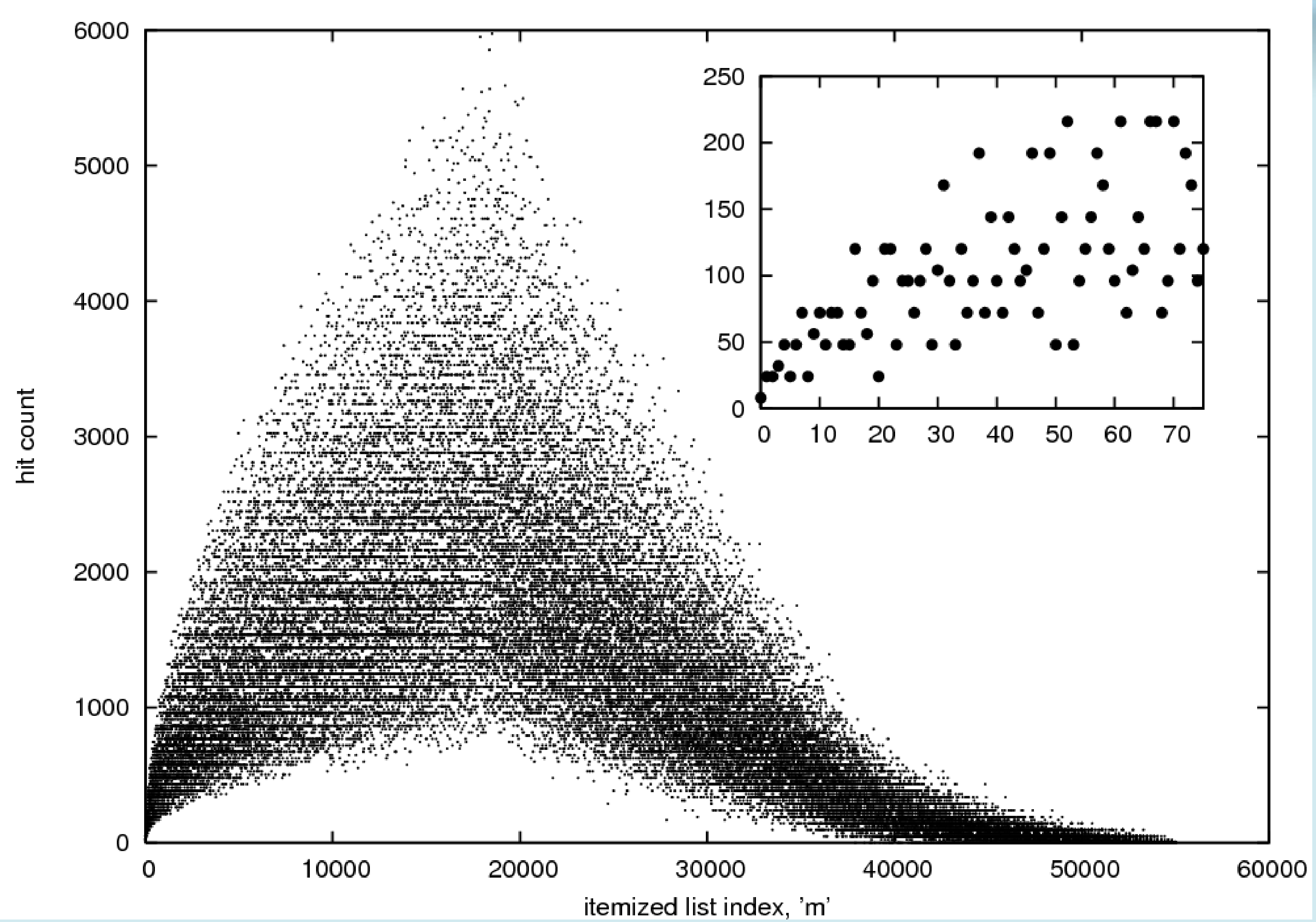

Spherical Average Operator

- We note that every Cartesian cell center must be at a radius r_m from the center of the star (m is an integer):

$$r_m = \Delta x \sqrt{0.75 + 2m}$$

- Procedure:
  1. Create an itemized list (an irregularly spaced radial array) with every possible distance a Cartesian cell center could map to.
  2. Collect the average over all Cartesian cell values that map into each itemized list index.
  3. Quadratic interpolation from the itemized list onto the base state array.

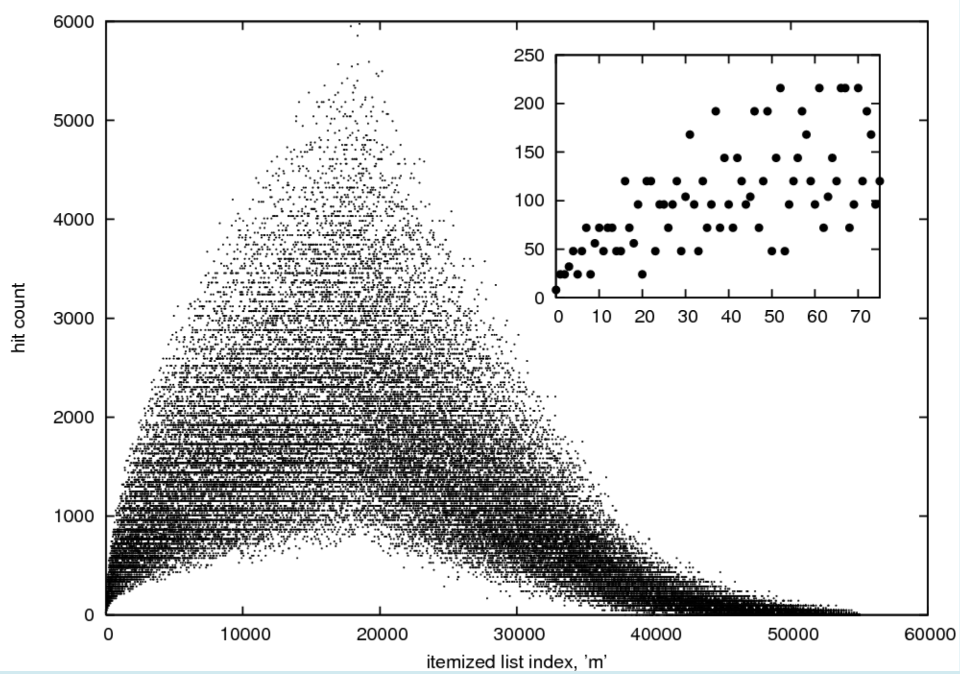

Spherical Average Operator

- Our new averaging procedure gives a relative error of at most $O(10^{-8})$.

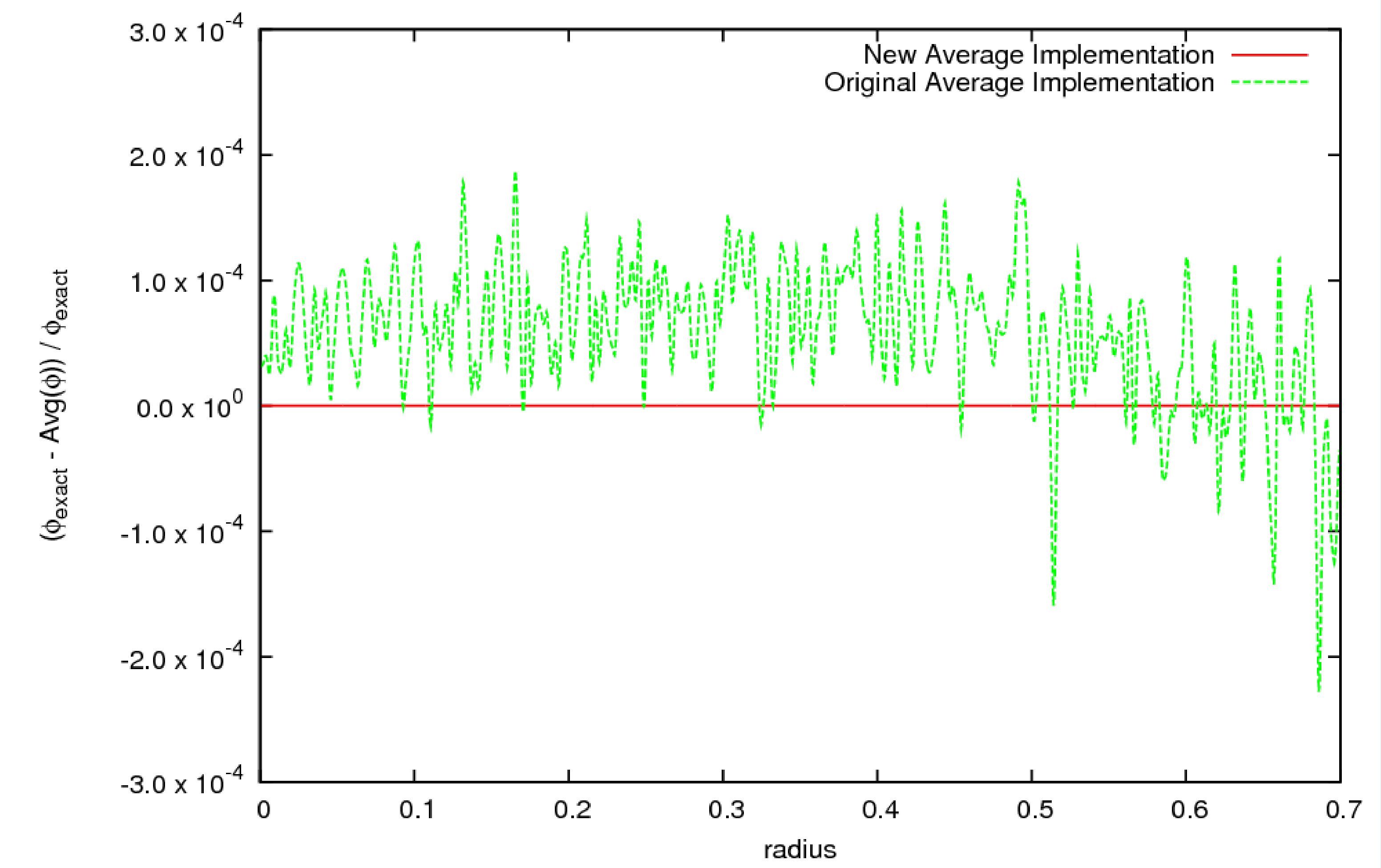

Adaptive Mesh Refinement

- Incorporate AMR using established techniques
  - Advance each level independently and synchronize fluxes, velocities, and pressure at coarse-fine interfaces
- For the full star problem, we need to consider our tagging criteria
  - Burning occurs in center of the star, driving convection in the inner part of the star.
  - We expect ignition point(s) to be near the center of the star

Adaptive Mesh Refinement

- 5000 km^3 domain
- 576^3 resolution
  - $1728 \cdot 48^3$ grids
  - 8.7 km resolution

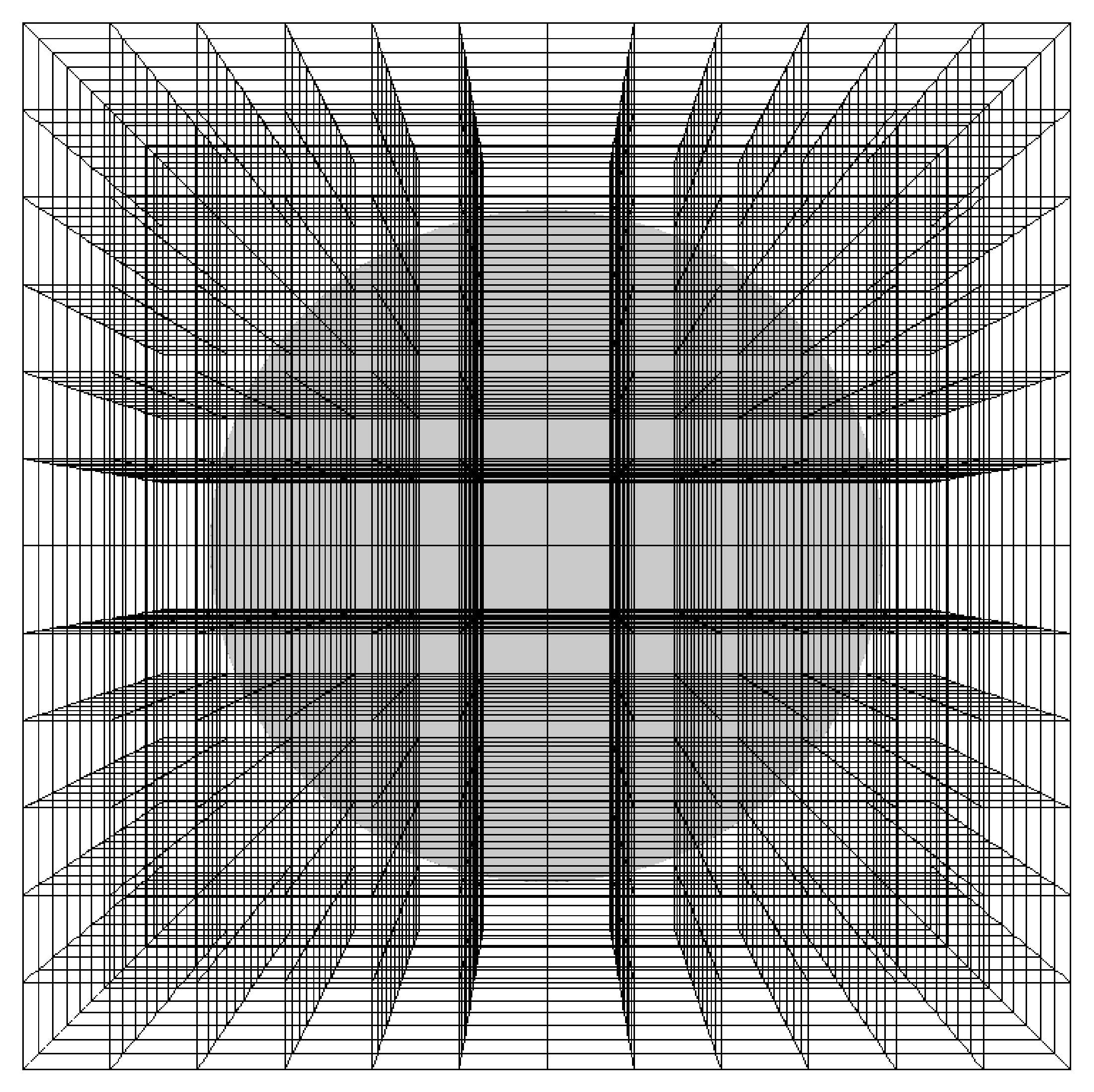

Adaptive Mesh Refinement

- 5000 km^3 domain
- 576^3 resolution
  - 1728 · 48^3 grids
  - 8.7 km resolution
- 1152^3 resolution
  - 1831 grids

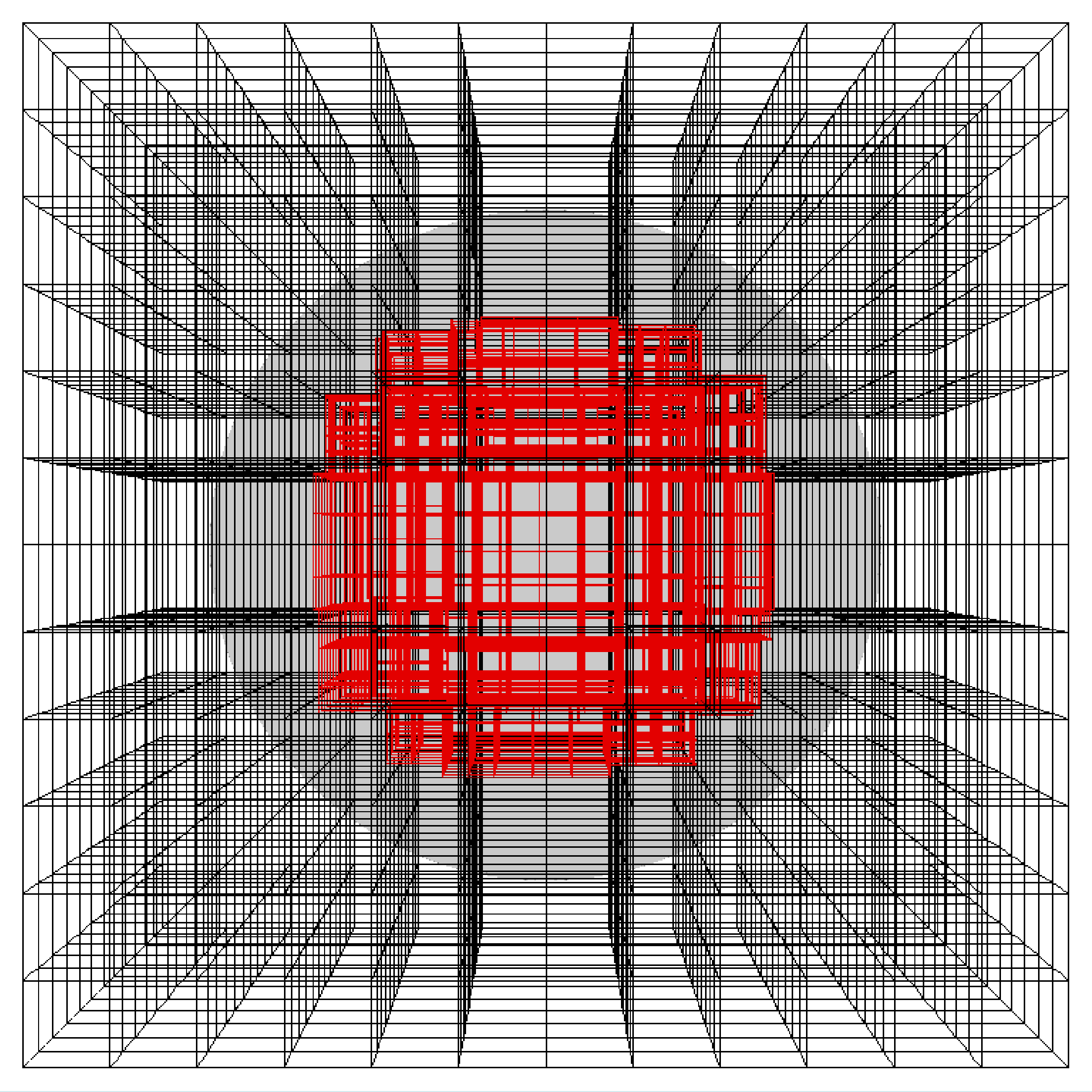

Adaptive Mesh Refinement

- 5000 km^3 domain
- 576^3 resolution
  - $1728 \cdot 48^3$ grids
  - 8.7 km resolution
- 1152^3 resolution
  - 1831 grids

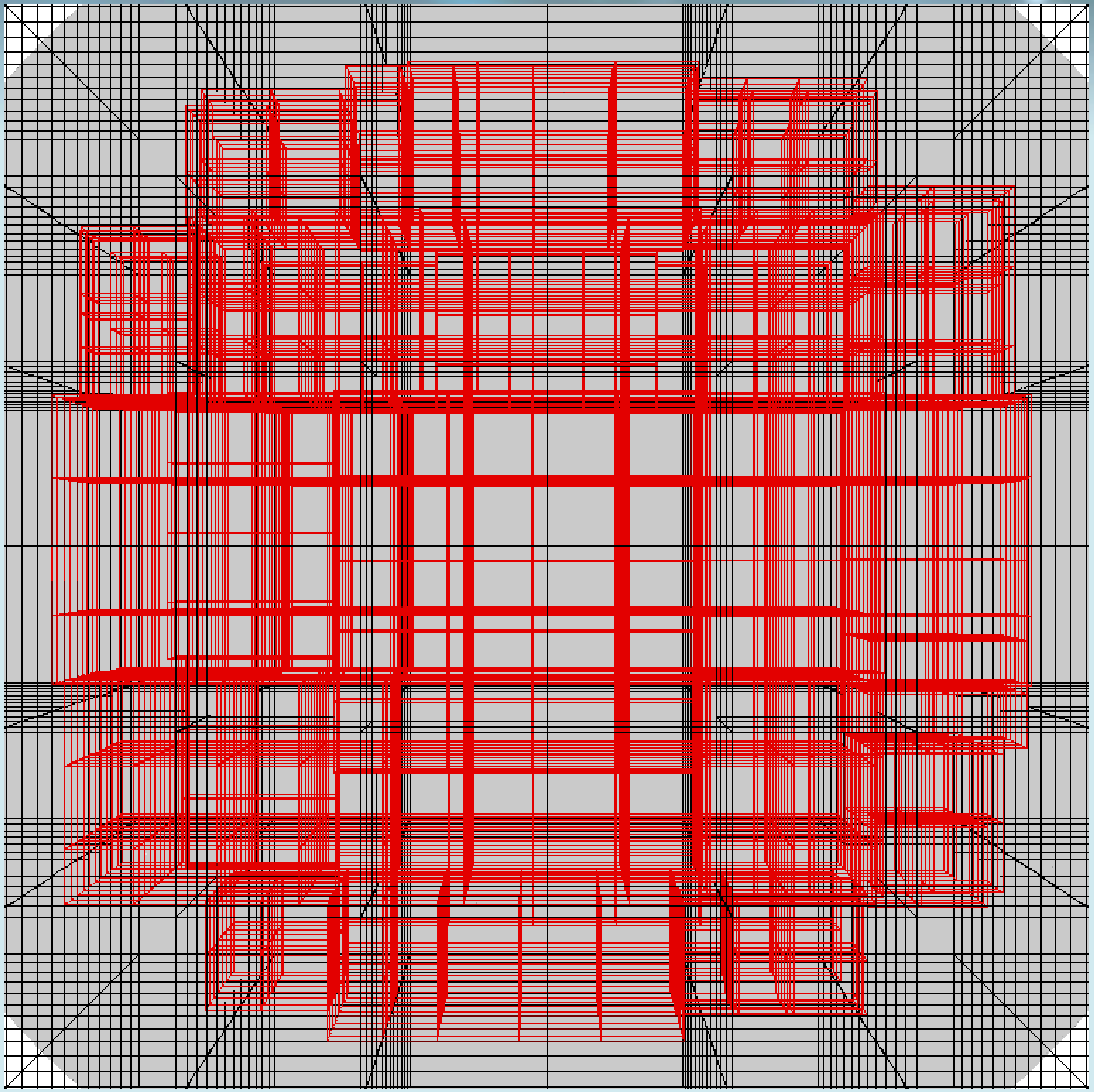

Adaptive Mesh Refinement

- 5000 km^3 domain
- 576^3 resolution
  - $1728 \cdot 48^3$ grids
  - 8.7 km resolution
- 1152^3 resolution
  - 1831 grids
- 2304^3 resolution
  - 2449 grids
- 4608^3 resolution
  - 7072 grids
  - 1.1 km resolution

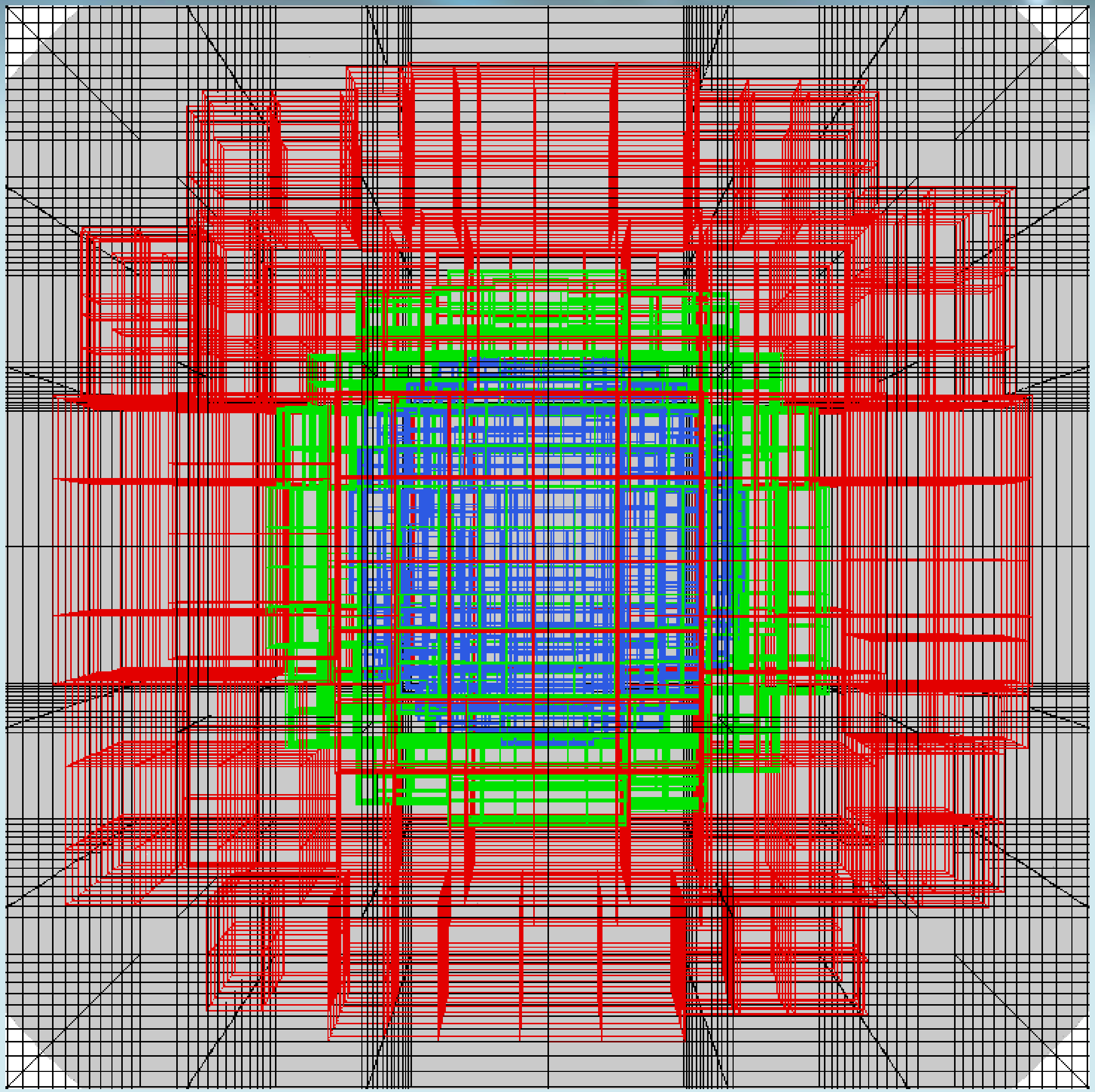

Adaptive Mesh Refinement

- 5000 km^3 domain
- 576^3 resolution
  - $1728 \cdot 48^3$ grids
  - 8.7 km resolution
- 1152^3 resolution
  - 1831 grids
- 2304^3 resolution
  - 2449 grids
- 4608^3 resolution
  - 7053 grids
  - 1.1 km resolution

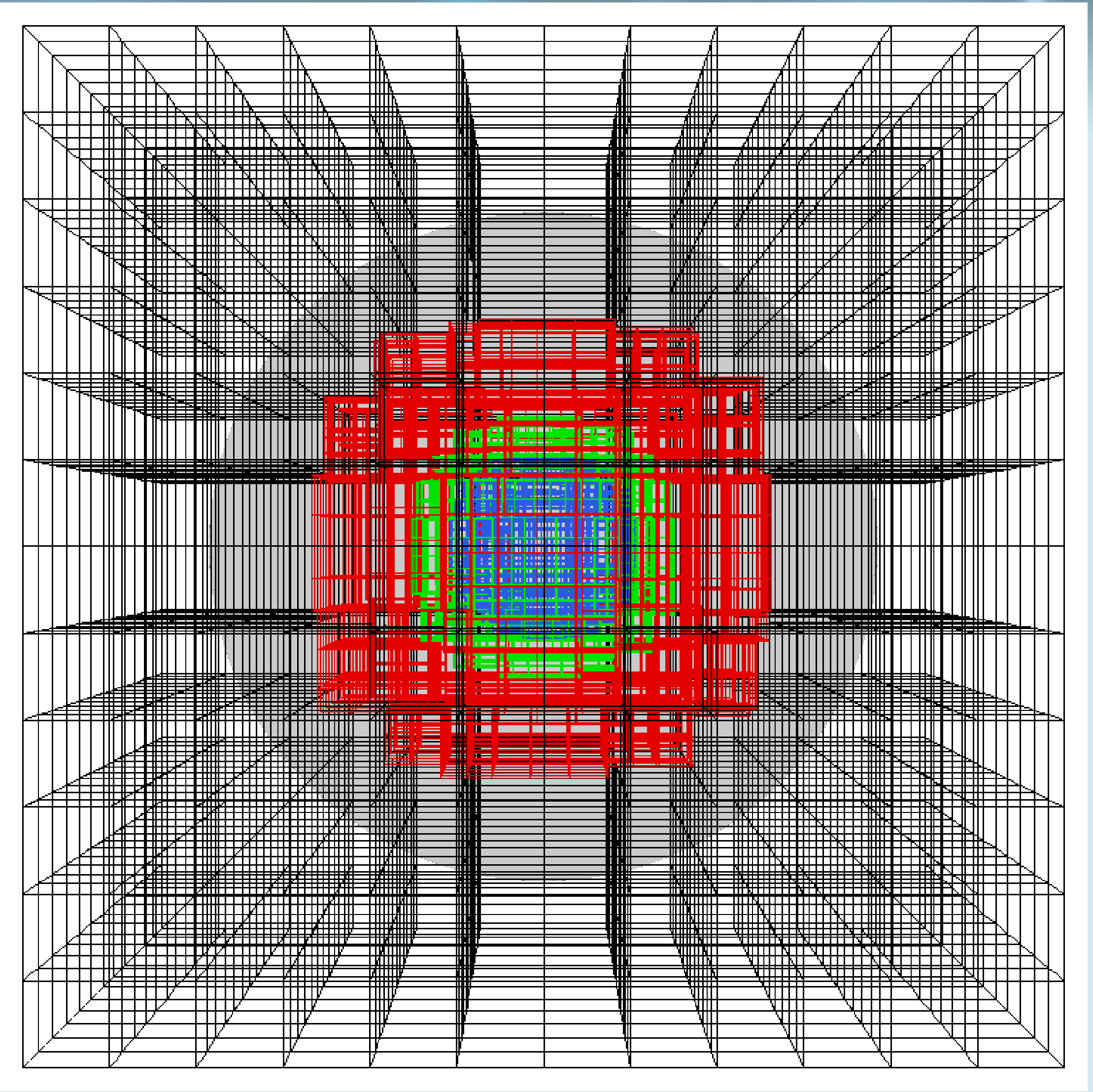

AMR Average Operator

- Primary new difficulty it the average operator - base state mapping from 3D to 1D

– The planar average operator is still straightforward

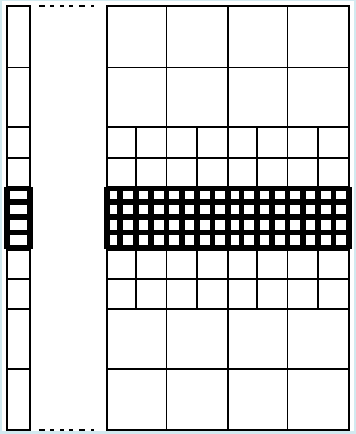

– The spherical average operator becomes more complicated

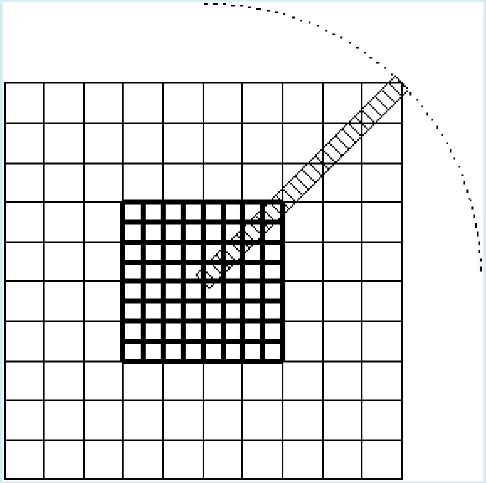

Note that the 1D radial array still has a constant spacing of $\Delta r = (1/5)\ \Delta x_{finest}$

AMR Spherical Average Operator

- Compute an itemized list for each level of refinement

$$r_m^l = \Delta x^l \sqrt{0.75 + 2m}$$

- When computing the average, select interpolation points from only one list, which is chosen by determining the list with the largest minimum hit count over the proposed interpolation points.
  - Merging the lists together into a “master list” causes large spikes in relative error near coarse-fine interfaces.

- We performed our average test using the following 3-level AMR grid structure:
  - The relative error was still $O(10^{-8})$.

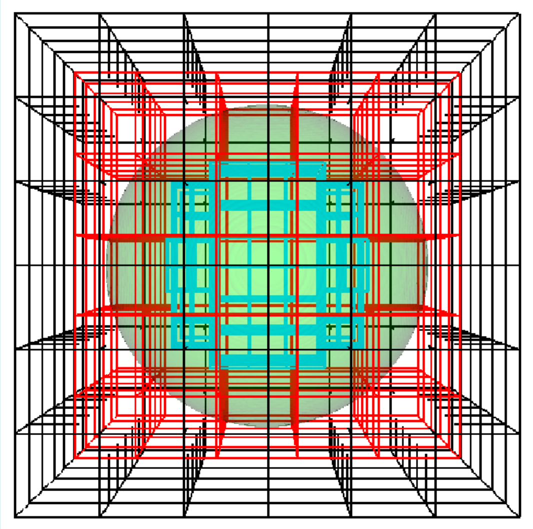

Parallelization Strategy

- We have recently adopted a hierarchical programming model, using a hybrid MPI/OpenMP approach to parallelization.

MPI Parallel Implementation

- Divide solution domain into grids

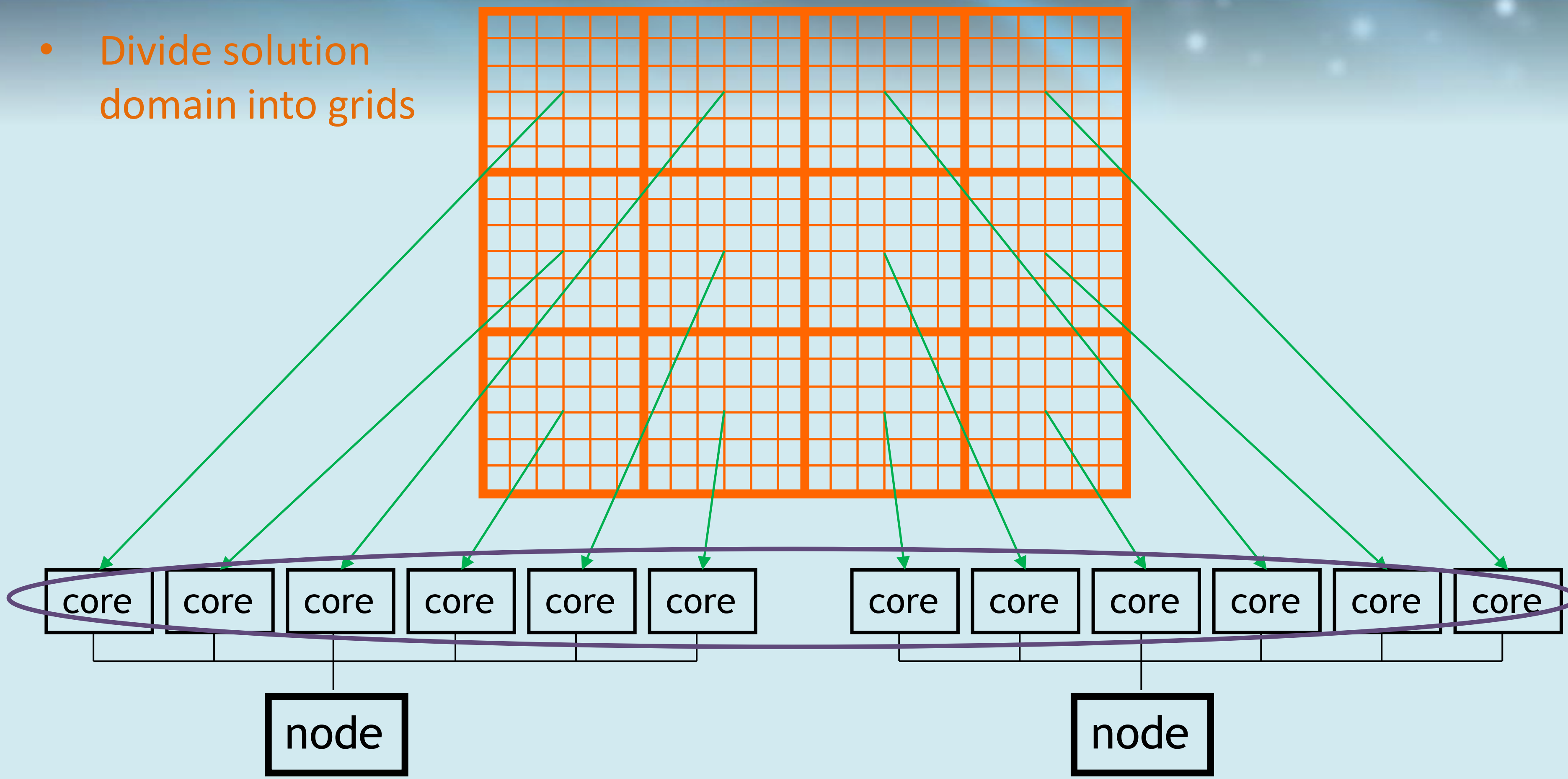

- Each grid is assigned to a core
- Cores communicate each other using MPI
  - In this example, we require 12 MPI processes.

Hybrid MPI/OpenMP Parallel Implementation

- Divide solution domain into fewer, larger grids

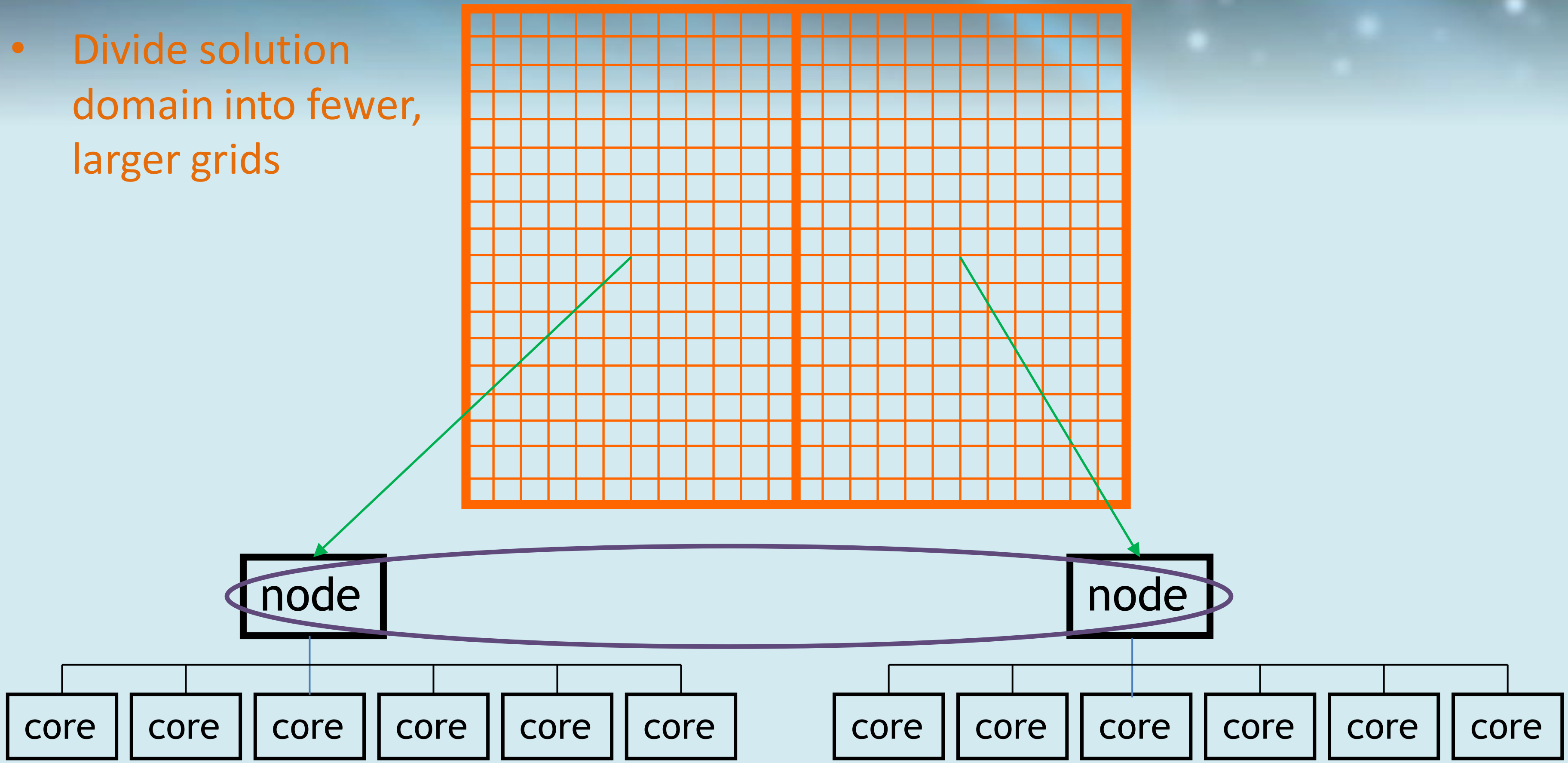

- Each grid is assigned to a node
  - Spawn a thread on each core to work on the grids simultaneously
- Nodes communicate each other using MPI
  - In this example, we require 2 MPI processes.

Advantages of Hybrid Parallel Implementation

- Fewer MPI processes lead to reduced communication time
  - Especially important in communication-intensive multigrid
- Fewer grids leads to reduced memory overhead requirements

MAESTRO Strong Scaling

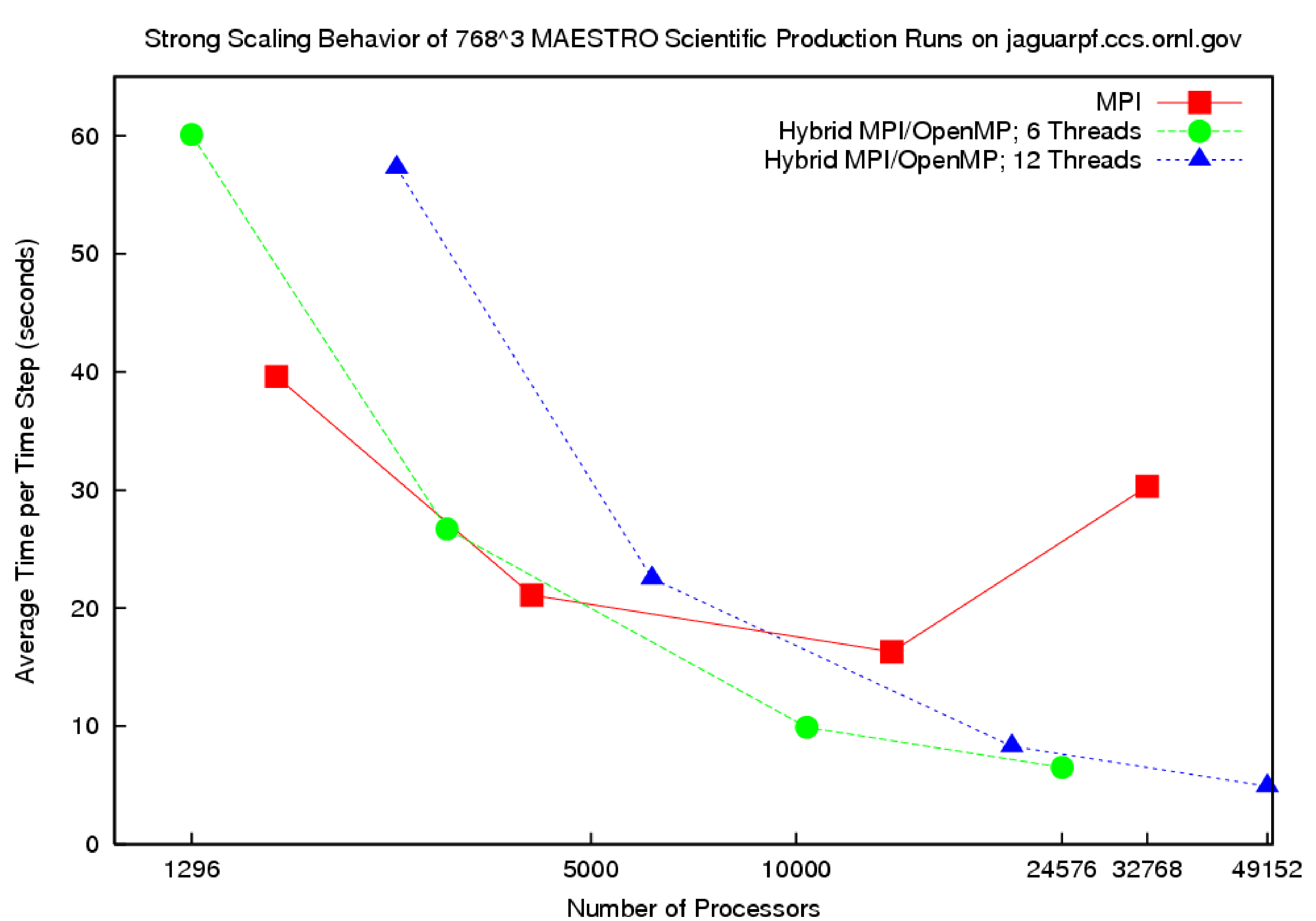

MAESTRO Weak Scaling

- Weak scaling results for a 2-level Type Ia supernovae simulation.

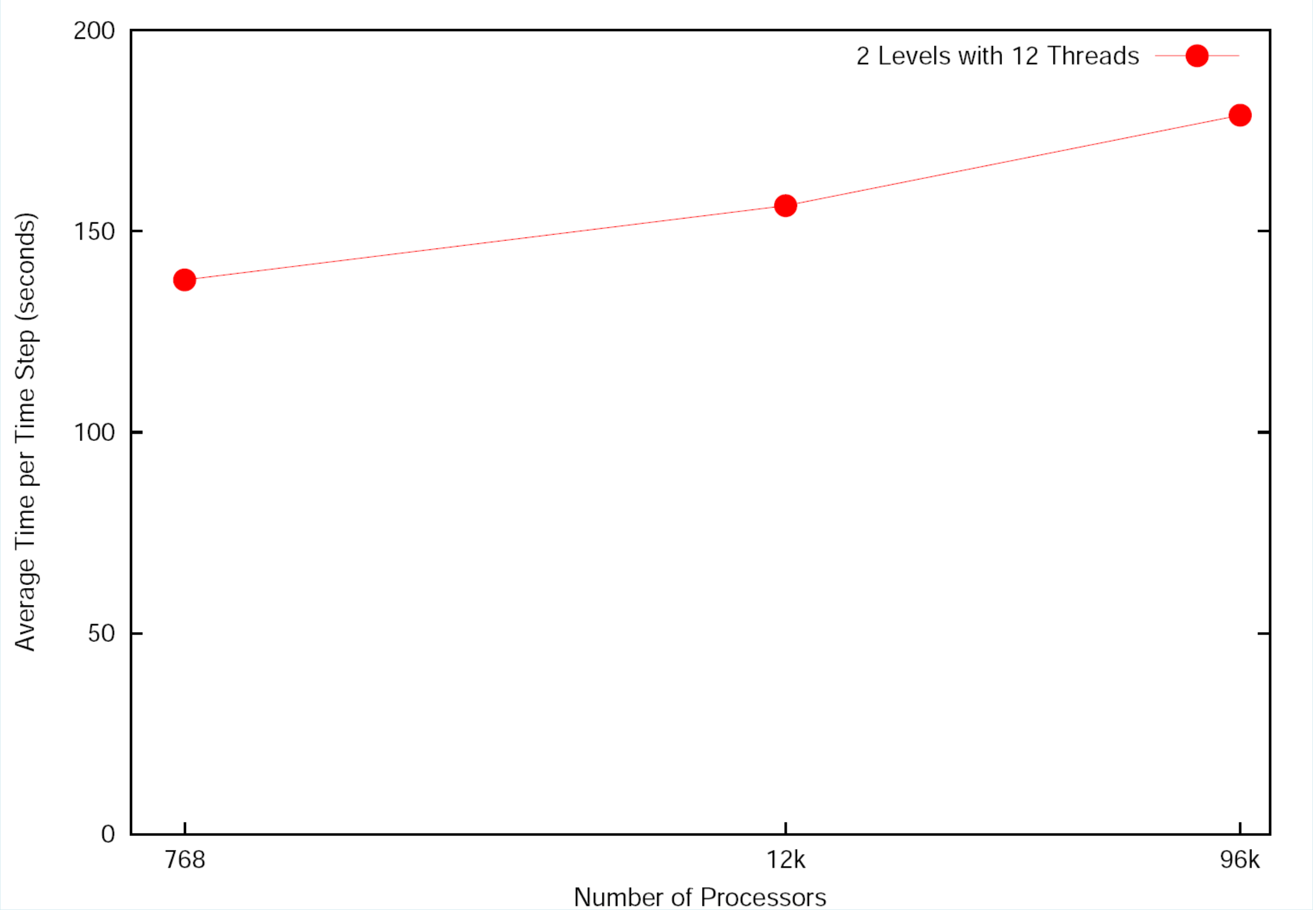

CASTRO Weak Scaling

- Using weak scaling, CASTRO compressible code scales to 200,000+ cores for the full white dwarf problem

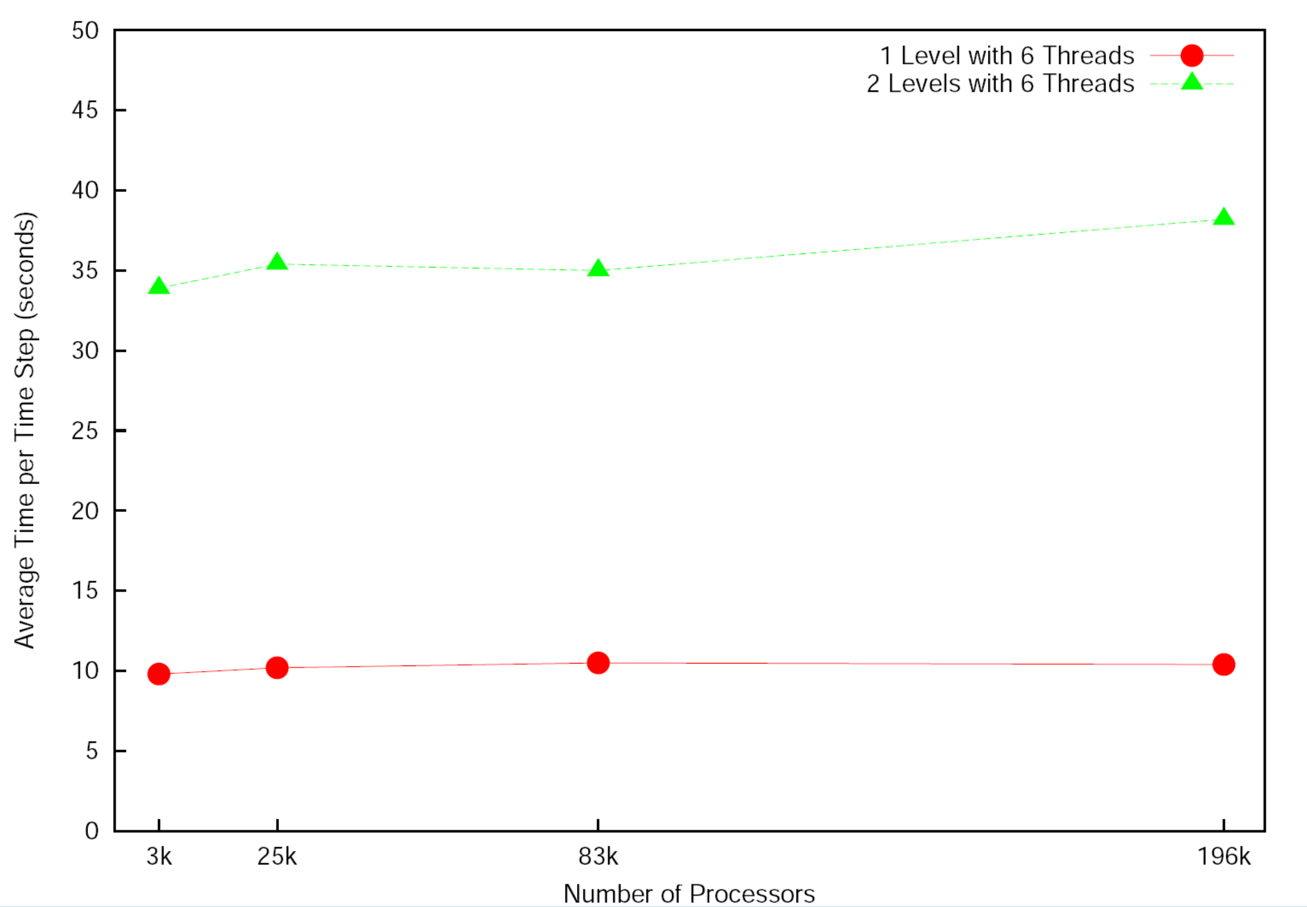

MAESTRO: Low Mach Number Astrophysics

- Scientific Results

White Dwarf Convection

- We have already performed several moderate-resolution simulations up to ignition with AMR. (up to 4.3km resolution)

- Some key results
  - Obtained 2+ hours of convective patterns leading to ignition
  - Determined likely ignition radii

White Dwarf Convection

- Initial conditions
  - 1D KEPLER model mapped onto Cartesian grid
  - Random velocity perturbation added to prevent initial nuclear runaway

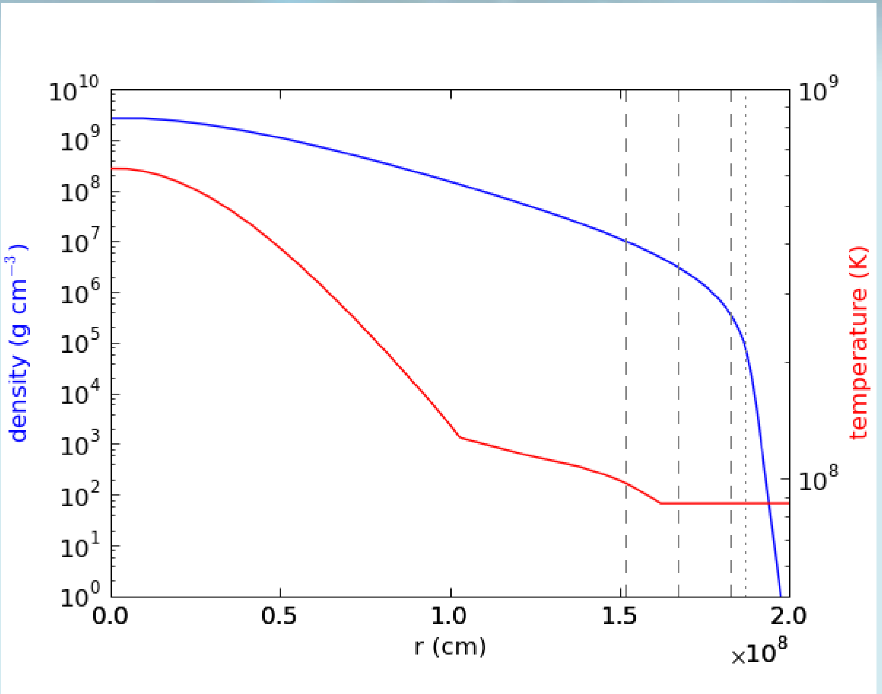

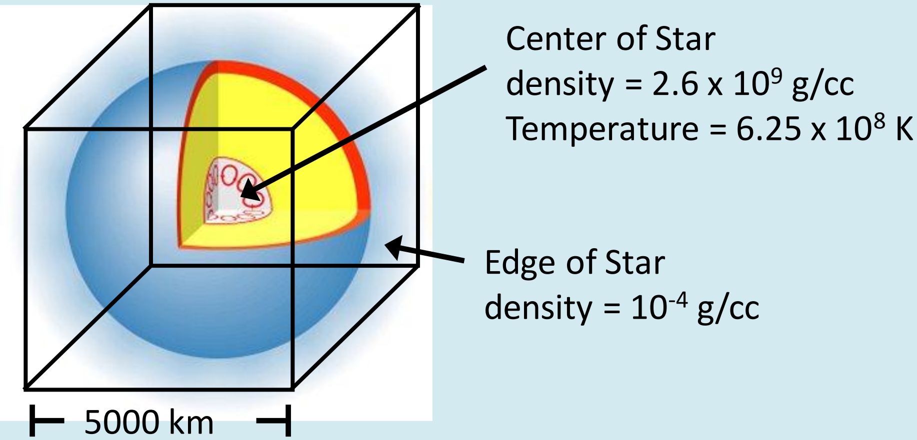

- We examine the convection in a non-rotating and slowly rotating (1.5% Keplerian) white dwarf.

White Dwarf Convection

- Red / Blue = outward / inward radial velocity
- Yellow / Green = contours of increasing burning rate

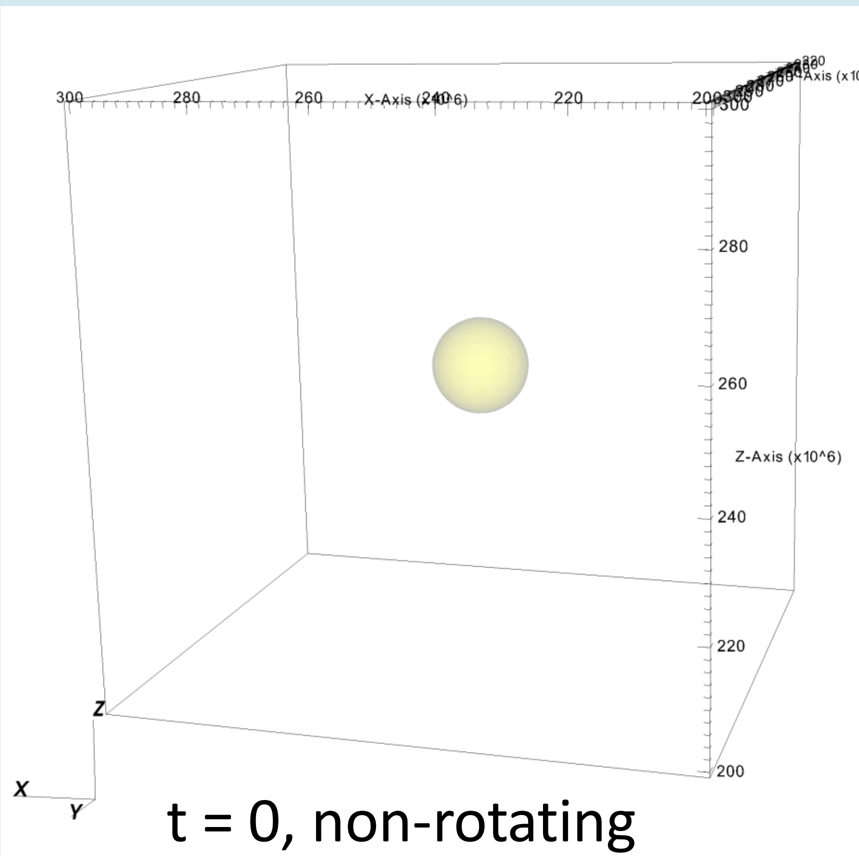

t = 0, non-rotating

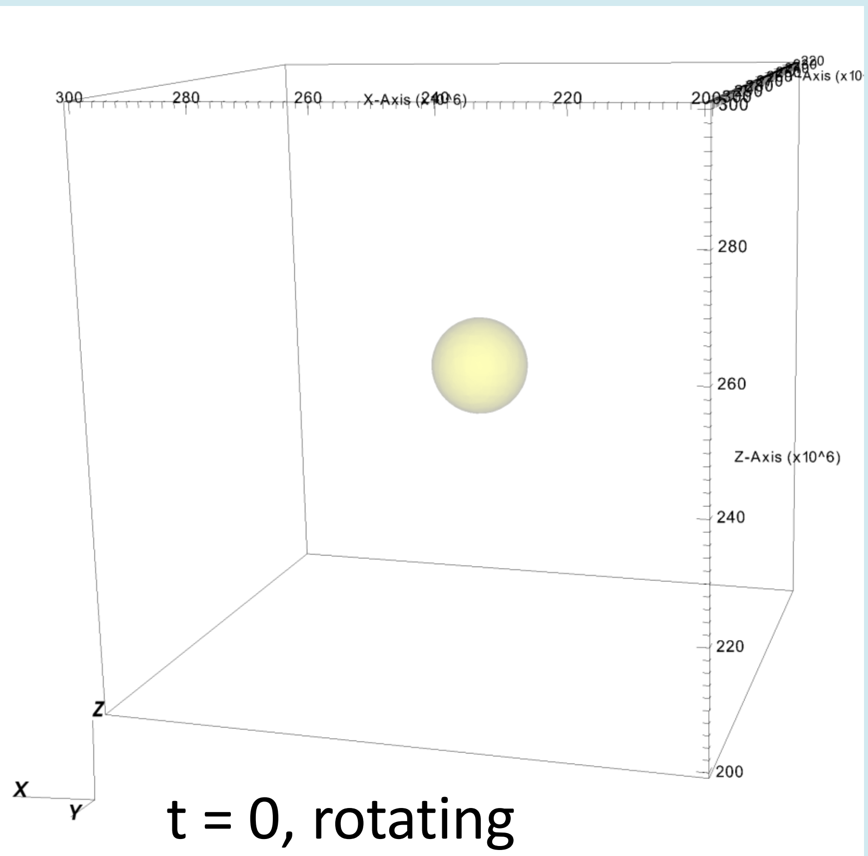

t = 0, rotating

White Dwarf Convection

- Red / Blue = outward / inward radial velocity
- Yellow / Green = contours of increasing burning rate

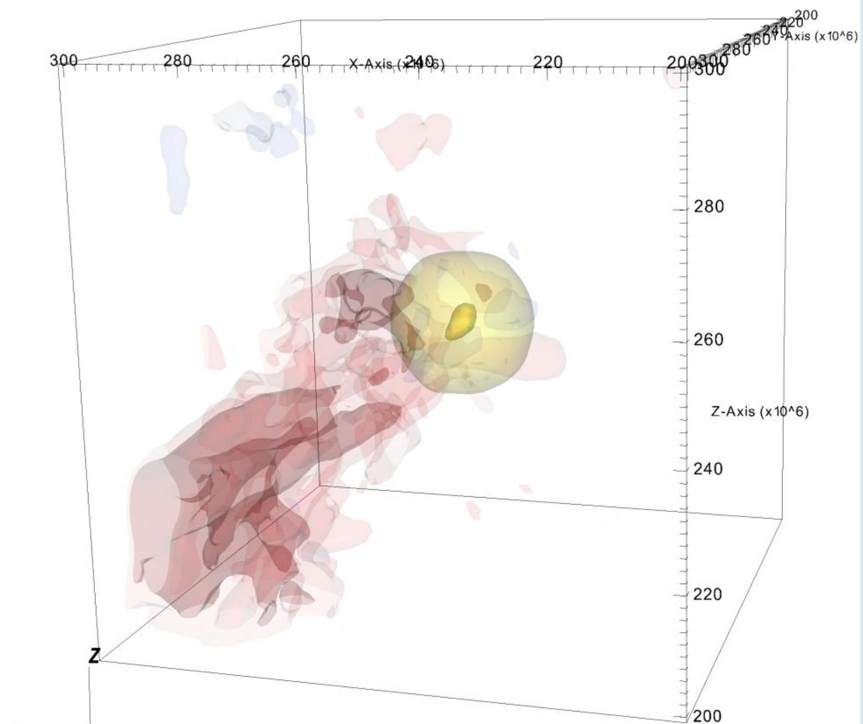

t = 1 hour, non-rotating

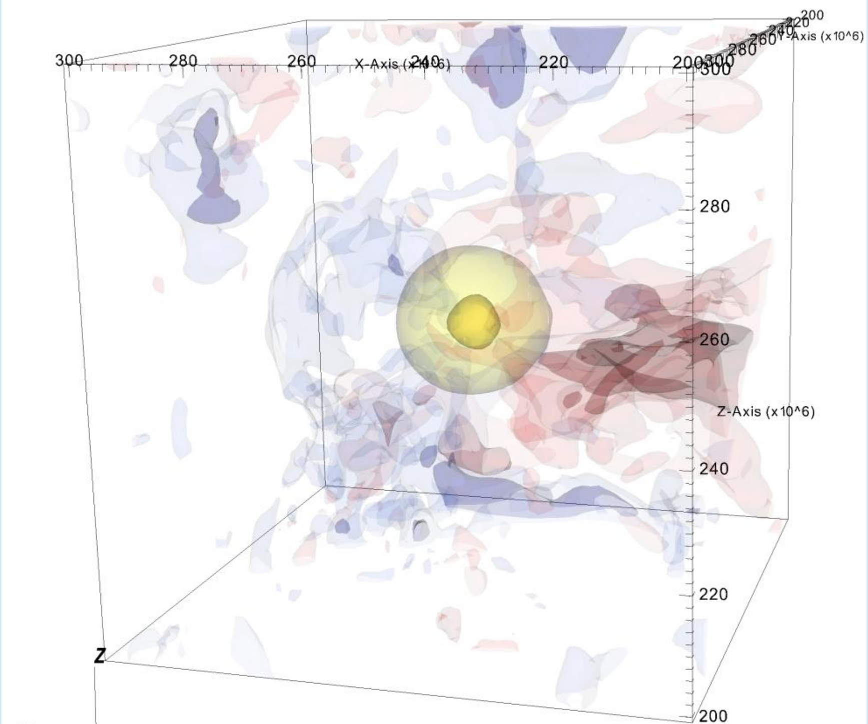

t = 1 hour, rotating

White Dwarf Convection

- Red / Blue = outward / inward radial velocity
- Yellow / Green = contours of increasing burning rate

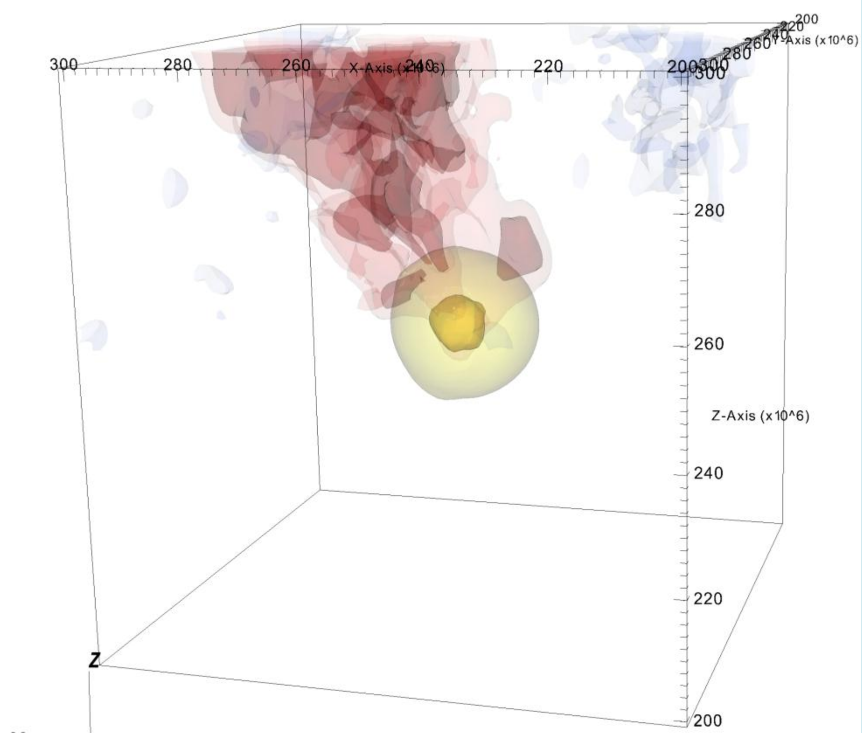

t = 1.25 hours, non-rotating

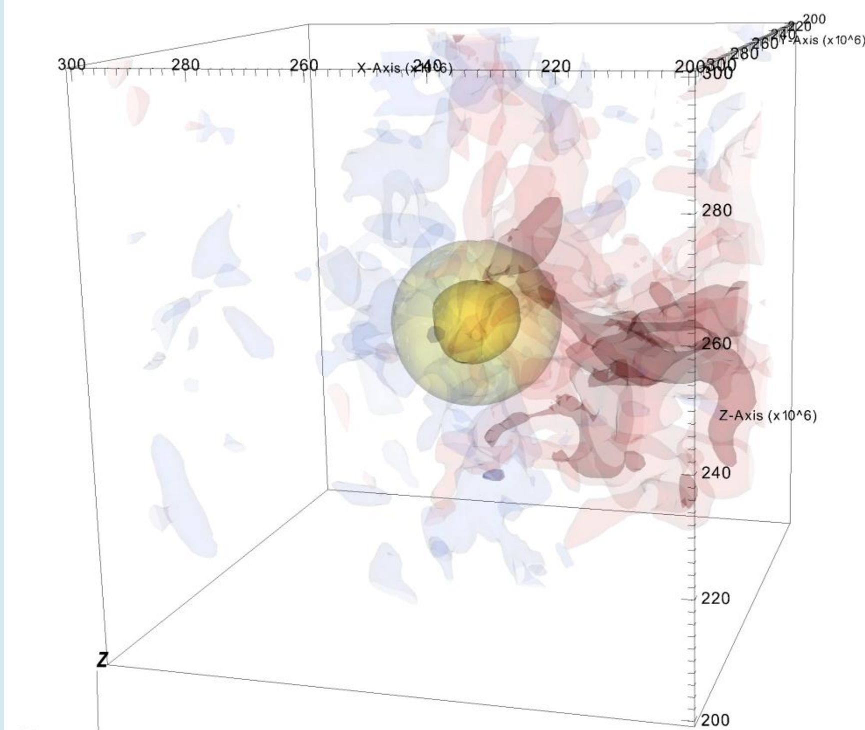

t = 1.25 hours, rotating

White Dwarf Convection

- Red / Blue = outward / inward radial velocity
- Yellow / Green = contours of increasing burning rate

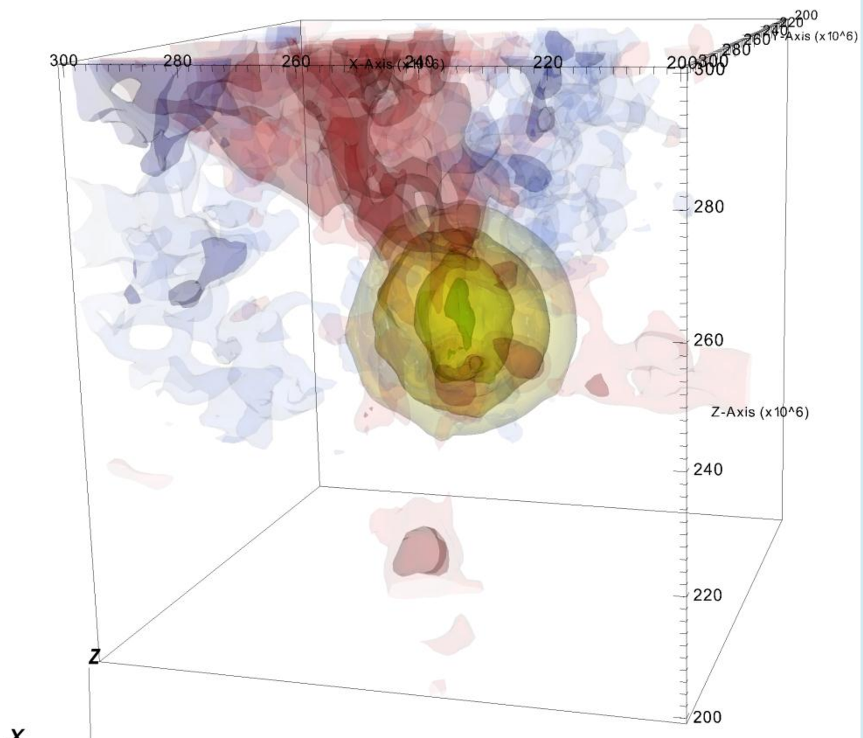

t = 2.25 hours, non-rotating

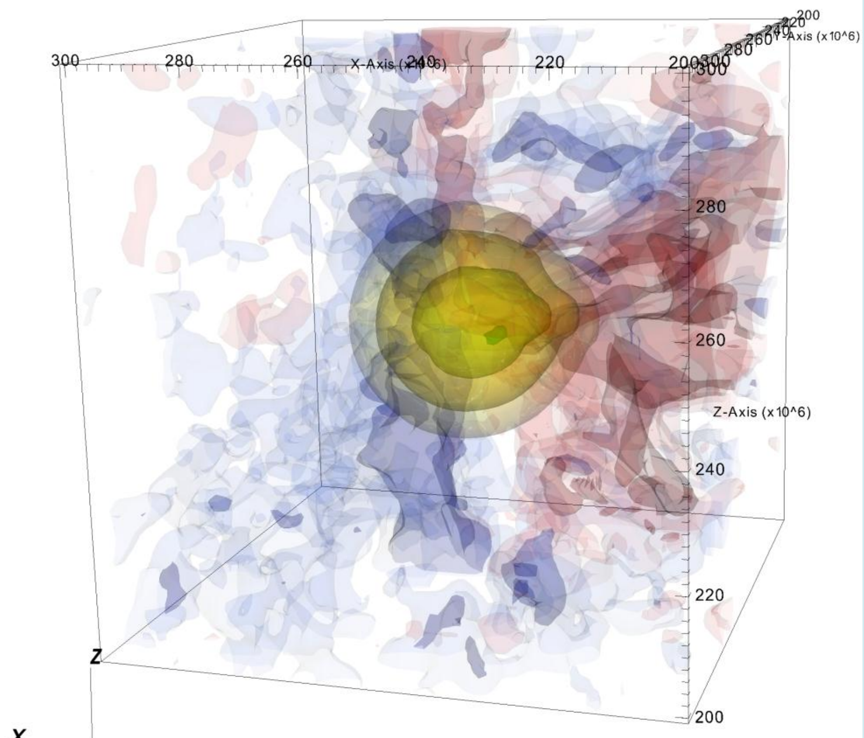

t = 2.75 hours, rotating

WD Convection: Long-Time Behavior

- Maximum temperature and Mach number over time.

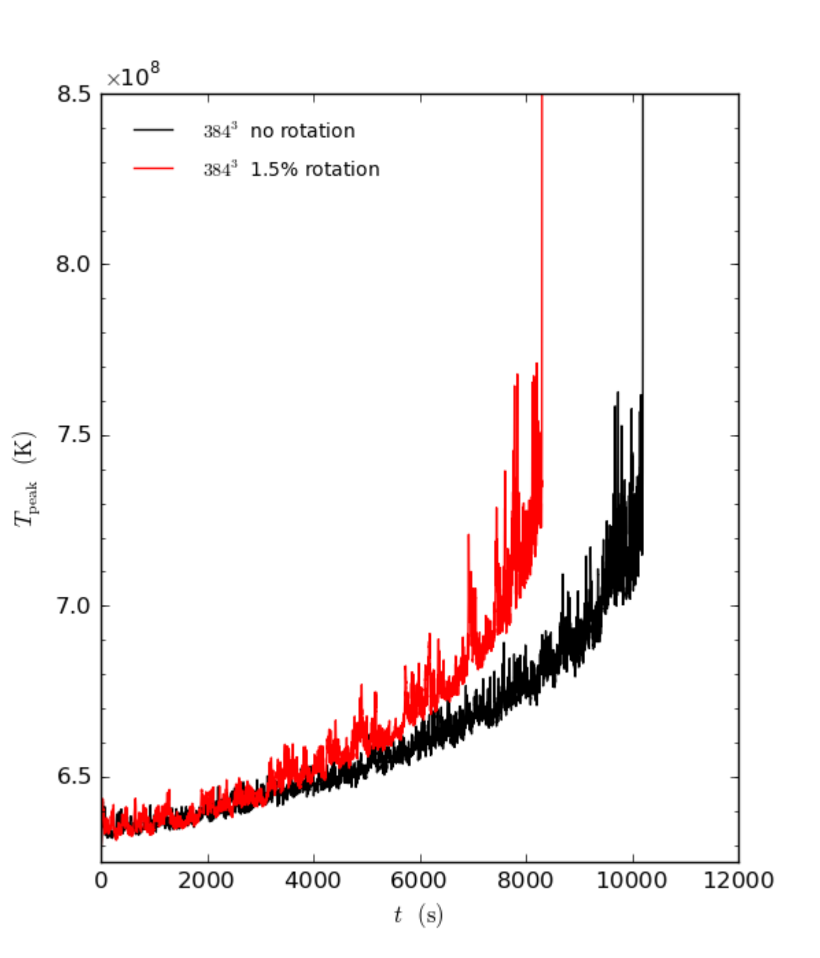

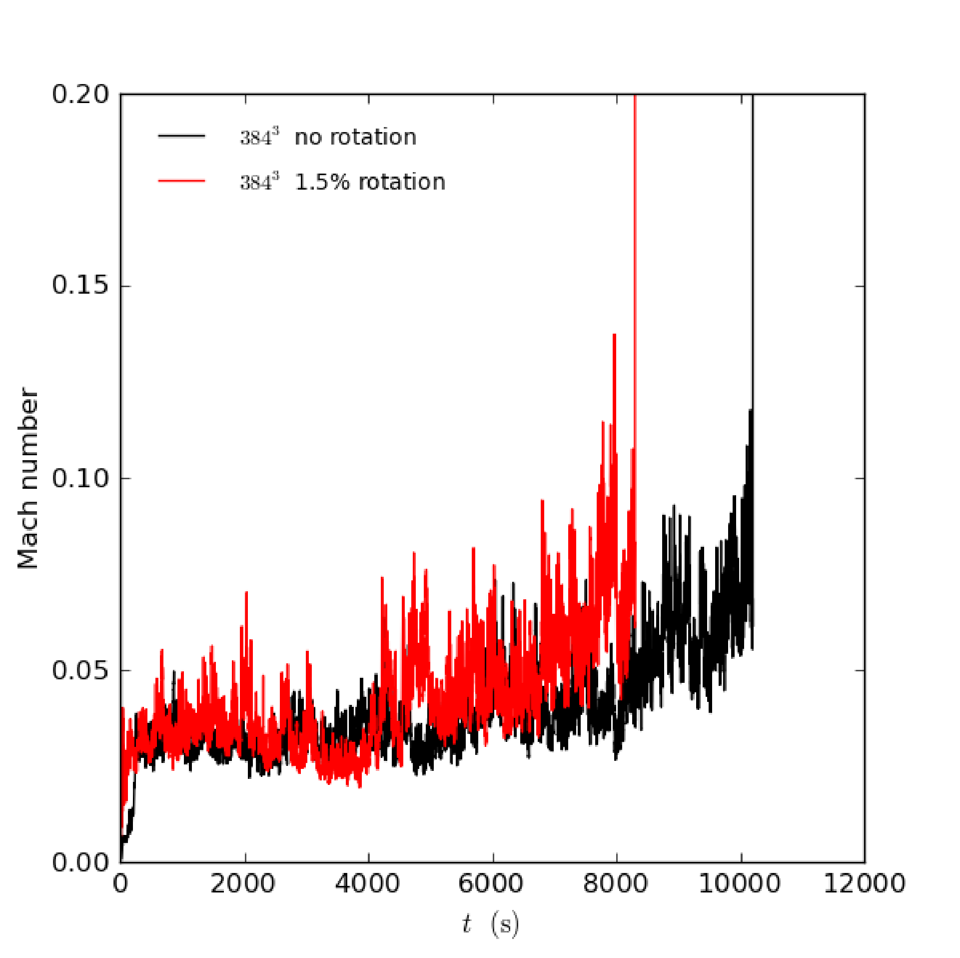

WD Convection: Ignition

- Last few seconds preceding ignition

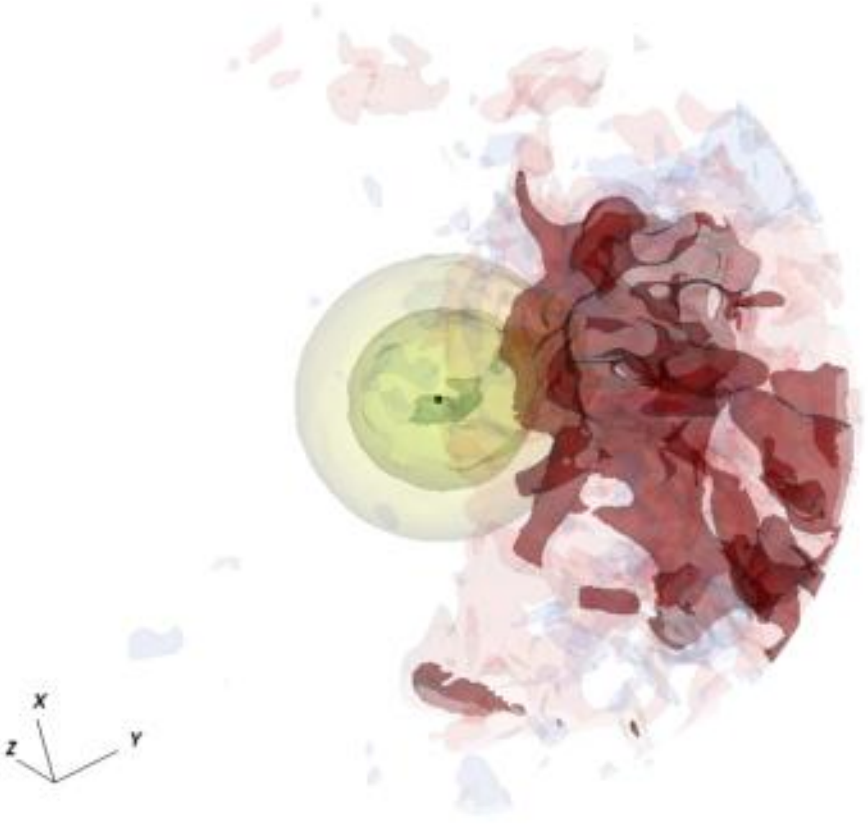

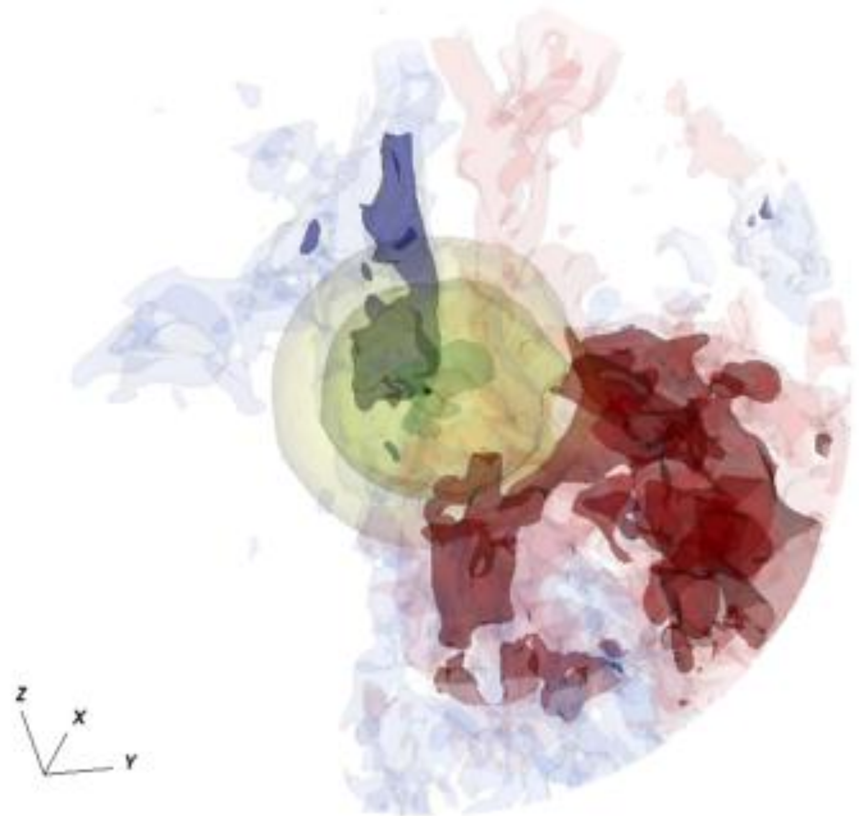

Non-rotating

Rotating

WD Convection: Ignition

- Examining the radius of the hot spot over the last few minutes indicates ignition radius of 50-70 km off-center is favored.

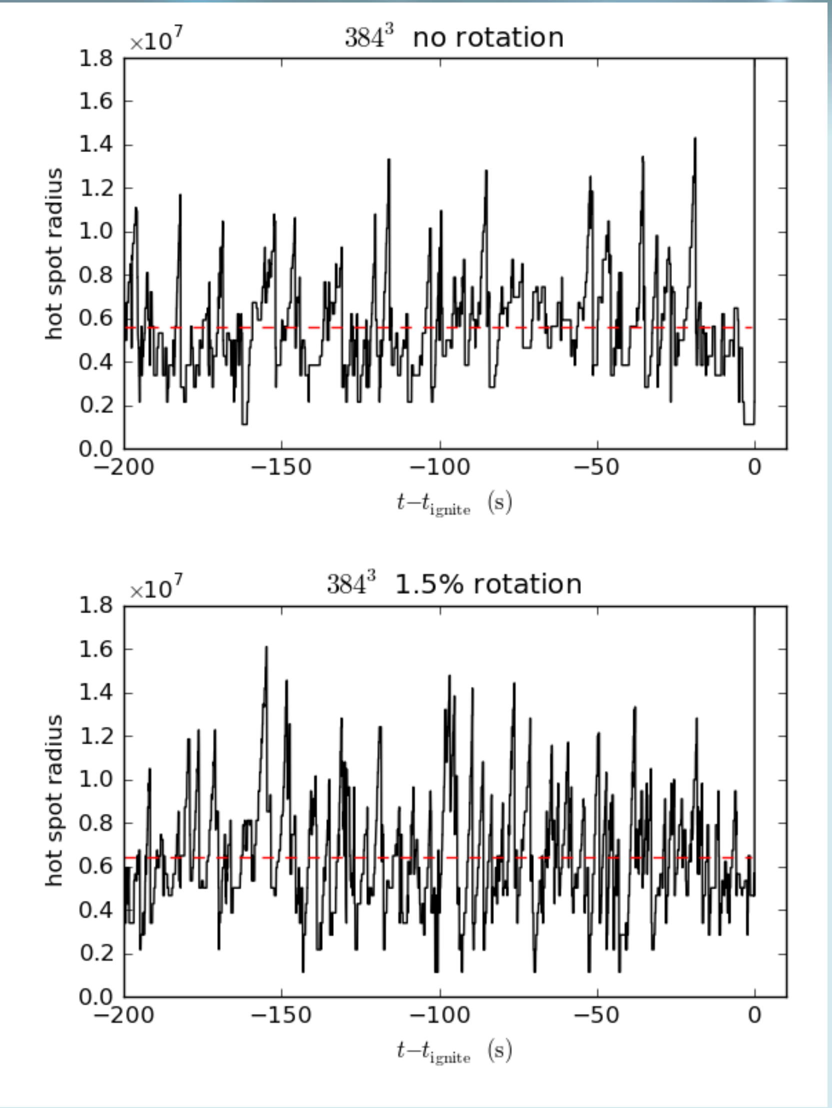

WD Convection: Ignition

- Histograms of ignition conditions over the final 200 seconds
  - (Left) Temperature and location of peak hot spot
  - (Right) Radial velocity and location of peak hot spot

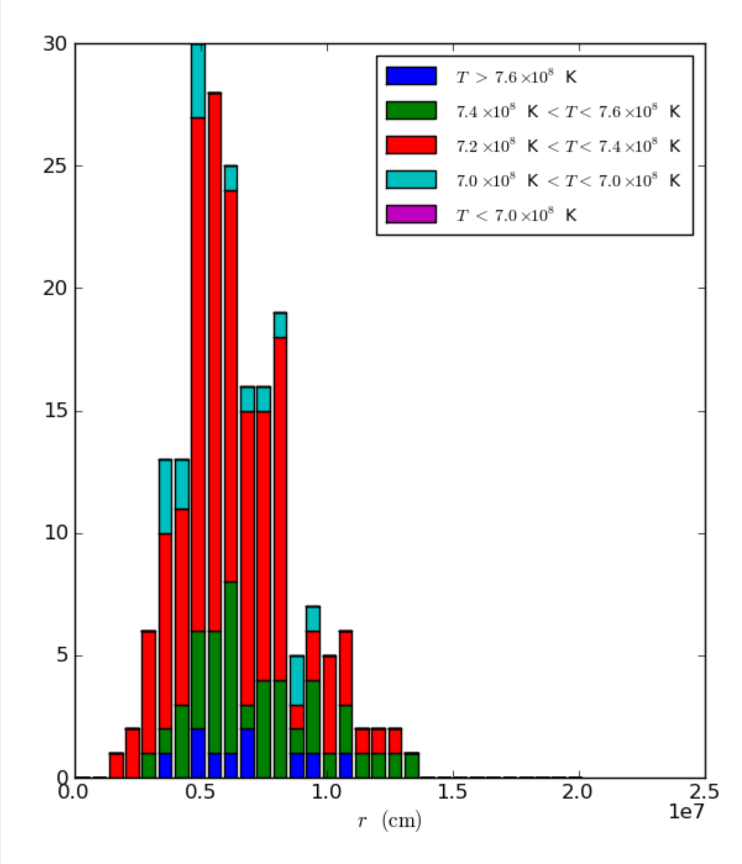

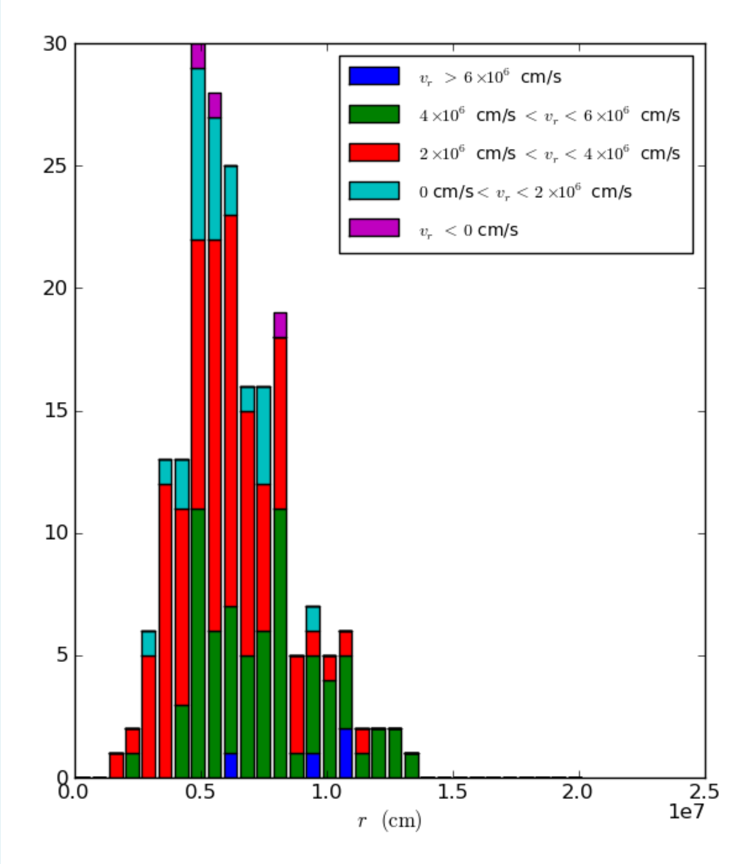

MAESTRO: Low Mach Number Astrophysics

- Transition to Compressible Framework

CASTRO Overview

- CASTRO is a massively parallel, finite volume, general compressible AMR hydrodynamics solver for astrophysical phenomena. (C++/Fortran90 BoxLib)

$$\begin{aligned}
\frac{\partial(\rho X_k)}{\partial t} &= -\nabla \cdot (\rho X_k \mathbf{u}) + \rho \dot{\omega}_k \\
\frac{\partial(\rho \mathbf{u})}{\partial t} &= -\nabla \cdot (\rho \mathbf{u}\mathbf{u}) - \nabla p + \rho \mathbf{g} \\
\frac{\partial(\rho E)}{\partial t} &= -\nabla \cdot (\rho \mathbf{u} E + p \mathbf{u}) + \rho \mathbf{u} \cdot \mathbf{g} + \nabla \cdot k_{\mathrm{th}} \nabla T + \rho H
\end{aligned}$$

- Compressible equations of motion
  - Explicit time evolution
  - Gravity can be computed with a Poisson solve (requires multigrid) or a monopole approximation (no multigrid)

MAESTRO to CASTRO Transition

- MAESTRO and CASTRO both use the BoxLib software libraries
  - Datasets compatible; we are able to initialize a CASTRO simulation from MAESTRO data.

- But there are still unresolved issues.
  - One of these issues is the role of pressure.
    - How does MAESTRO $p_0 + \pi$ compare to the CASTRO pressure?
    - What about higher-order terms in Mach number we ignored in the derivation of the MAESTRO equations?

MAESTRO to CASTRO Transition

- Study the effects of using a MAESTRO dataset to initialize a CASTRO simulation
  - Different initialization algorithms
  - Mach number dependency
  - EOS dependency

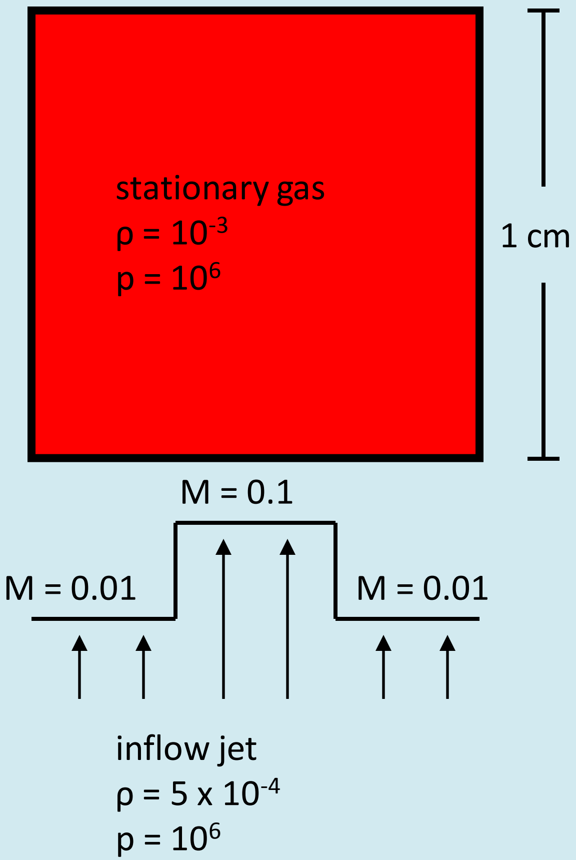

- Test problem description
  - Gamma-law gas, terrestrial conditions
  - Subsonic inflow jet with lower density

Density evolution

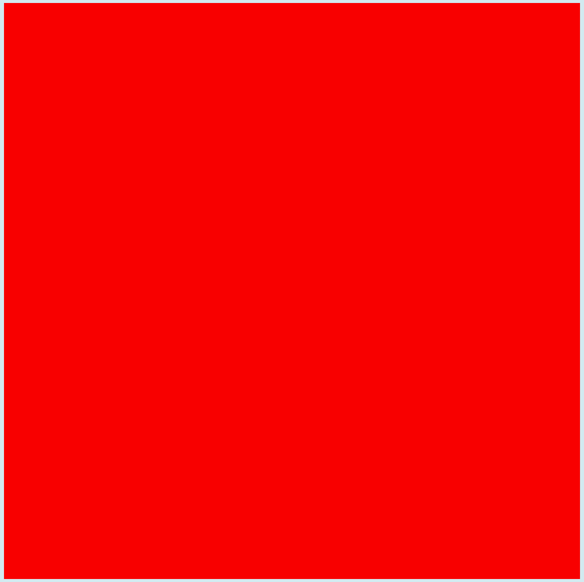

MAESTRO pressure evolution

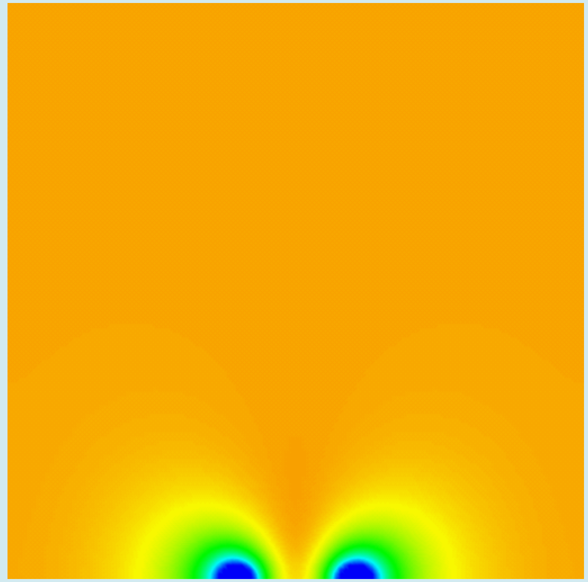

CASTRO pressure evolution

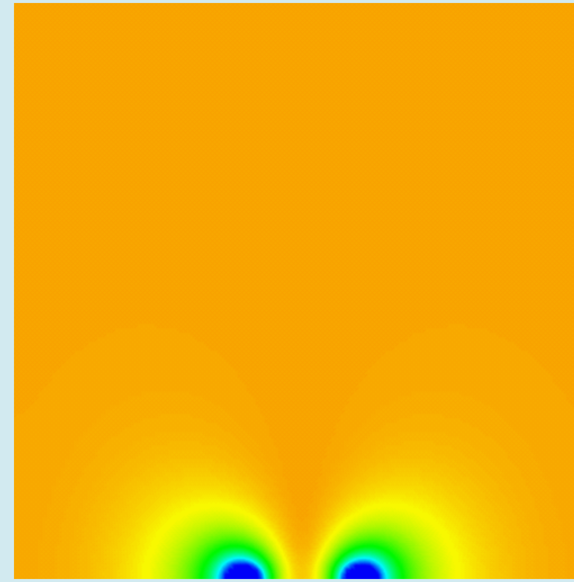

We restart the simulation in CASTRO with this profile

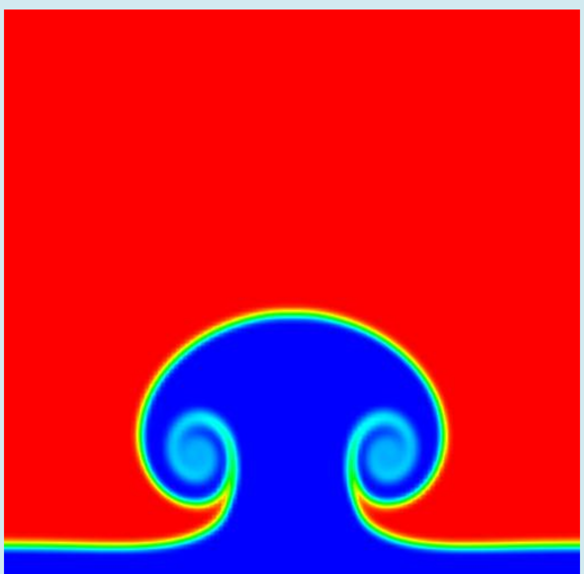

CASTRO pressure after initializing with $e = e(\rho,p_0)$

CASTRO pressure after initializing with $e = e(\rho,p_0+\pi)$

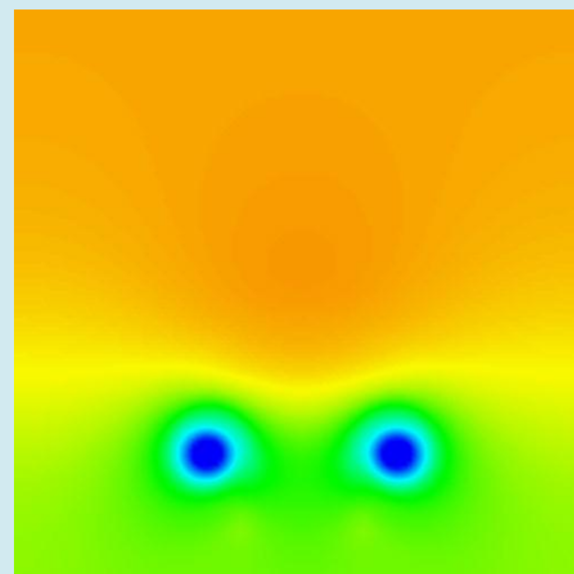

Future Work

- End-to-end Simulations using CASTRO and SEDONA
  - Currently running 2 km zone simulations in MAESTRO (current results at 4 km; ultimate goal is 1 km zone simulations) for CASTRO initial conditions.
- More accurate asymptotic models to explore higher-order behavior in Mach number
- Higher-order discretizations in space and time.
- Implementation strategies for multicore architectures
- Support scientific efforts of our growing user base.
  - AMR for Type I X-Ray Bursts (Chris Malone, Stony Brook)
  - Convection in Massive Stars (Candace Gilet, LBL/UCB)